Department of Energy

Washington, DC 20585

QA: N/A

DOCKET NUMBER 63-001

November 24, 2009

ATTN: Document Control Desk
John H. (Jack) Sulima, Project Manager
Project Management Branch Section B
Division of High-Level Waste Repository Safety
Office of Nuclear Material Safety and Safeguards
U.S. Nuclear Regulatory Commission
EBB-2B2
11545 Rockville Pike
Rockville, MD 20852-2738

YUCCA MOUNTAIN - REQUEST FOR ADDITIONAL INFORMATION - SAFETY EVALUATION REPORT, VOLUME 3, CHAPTER 2.2.1.2.1 (SCENARIO ANALYSIS), 6TH SET (DEPARTMENT OF ENERGY'S SAFETY ANALYSIS REPORT SECTION 2.2, TABLE 2.2-5)

Reference: Ltr, Sulima to Williams, dtd 10/14/09, "Yucca Mountain – Request for Additional Information – Safety Evaluation Report, Volume 3, Chapter 2.2.1.2.1 (Scenario Analysis), 6th Set (Department of Energy's Safety Analysis Report Section 2.2, Table 2.2-5)"

The purpose of this letter is to transmit the U.S. Department of Energy's (DOE) response to one (1) of the six (6) Requests for Additional Information (RAI) identified in the above-referenced letter. The RAI response is provided as enclosure to this letter. DOE submitted the response to RAI Number 3 from this set on November 5, 2009; responses to RAIs Numbers 4 and 5 on November 17; and plans to submit the remaining RAIs from this set on or before December 9, 2009.

The DOE references cited in the RAI response have previously been provided with the License Application (LA), the LA update, or as part of previous RAI response. The reference provided with previous RAI response is identified within the enclosed response reference section.

There are no commitments in the enclosed RAI responses. If you have any questions regarding this letter, please contact me at (202) 586-9620, or by email to jeff.williams@rw.doe.gov.

Jeffrey R. Williams, Supervisor
Licensing Interactions Branch
Regulatory Affairs Division
Office of Technical Management

OTM:CJM-0129

NMSS25

Enclosure:

Response to RAI Volume 3, Chapter 2.2.1.2.1, Set 6, Number 1

cc w/encl:
J. C. Chen, NRC, Rockville, MD
J. R. Cuadrado, NRC, Rockville, MD
J. R. Davis, NRC, Rockville, MD
R. K. Johnson, NRC, Rockville, MD
A. S. Mohseni, NRC, Rockville, MD
N. K. Stablein, NRC, Rockville, MD
D. B. Spitzberg, NRC, Arlington, TX
J. D. Parrott, NRC, Las Vegas, NV
L. M. Willoughby, NRC, Las Vegas, NV
Jack Sulima, NRC, Rockville, MD
Christian Jacobs, NRC, Rockville, MD
Lola Gomez, NRC, Rockville, MD
W. C. Patrick, CNWRA, San Antonio, TX
Budhi Sagar, CNWRA, San Antonio, TX
Bob Brient, CNWRA, San Antonio, TX
Rod McCullum, NEI, Washington, DC
B. J. Garrick, NWTRB, Arlington, VA
Bruce Breslow, State of Nevada, Carson City, NV
Alan Kalt, Churchill County, Fallon, NV
Irene Navis, Clark County, Las Vegas, NV
Ed Mueller, Esmeralda County, Goldfield, NV
Ron Damele, Eureka County, Eureka, NV
Alisa Lembke, Inyo County, Independence, CA
Chuck Chapin, Lander County, Battle Mountain, NV
Connie Simkins, Lincoln County, Pioche, NV
Linda Mathias, Mineral County, Hawthorne, NV
Darrell Lacy, Nye County, Pahrump, NV
Jeff VanNeil, Nye County, Pahrump, NV
Joe Kennedy, Timbisha Shoshone Tribe, Death Valley, CA
Mike Simon, White Pine County, Ely, NV
K. W. Bell, California Energy Commission, Sacramento, CA
Barbara Byron, California Energy Commission, Sacramento, CA
Susan Durbin, California Attorney General's Office, Sacramento, CA
Charles Fitzpatrick, Egan, Fitzpatrick, Malsch, PLLC

RAI Volume 3, Postclosure Chapter 2.2.1.2.1, Sixth Set, Number 1:

> Demonstrate how the Voronoi block model appropriately represents the characteristics of the Topopah Spring lower lithophysal tuff, such that the potential for drift collapse is not underestimated.
>
> Basis: In the UDEC-Voronoi model, DOE concludes that 30 cm average block diameters with randomly oriented sides are representative of the randomly oriented internal discontinuities within the Topopah Spring lower lithophysal tuff. DOE characterizes the Topopah Spring lower lithophysal tuff as having primarily vertical fractures with spacings on order of several centimeters (BSC 2004, section 7.3.2). Although DOE concludes that the presence of lithophysal voids creates a generally isotropic rock mass (DOE, 2009, RAI-1), DOE did not provide information to show how such voids homogenized the potential effects of a vertical anisotropy in the rock mass.

1. RESPONSE

The locations and shapes of the lithophysae in the Topopah Spring Tuff lower lithophysal (Tptpll) unit are random (see Figure A-10 in Appendix A); similarly, most fractures in the unit are closely spaced and have trace lengths of 30 cm or less (BSC 2005, Figure B-5). The combined characteristics of the random locations and shapes of the lithophysae (e.g., see Appendix A, Figures A-4 to A-6 and A-9 to A-10), and the close spacings and short trace lengths of fractures, create a rock mass that is reasonably represented by a homogeneous model for predicting mechanical response in the Tptpll unit because the size of the internal structure and spacing of fractures is much smaller than the drift diameter (~10 to 30 cm versus 5.5 m). The presence of lithophysae will concentrate stresses under external loads and lead to preferential failure of the rock matrix between the randomly located lithophysae and along local fracture partings coincident with stress concentrations. The model results in an isotropic response to mechanical stress at the scale of a drift. Therefore, while anisotropy exists, its effect on the mechanical response is not significant. The Voronoi block model representation is appropriate based on the validation of the drift-scale modeling of lithophysal rock with the UDEC program (BSC 2004, Section 7.6).

1.1 EFFECTS OF LITHOPHYSAE AND FRACTURES ON THE FABRIC OF THE Tptpll

The characteristic lithostratigraphic features of the lower lithophysal zone of the Tptpll are lithophysae and fractures. Lithophysae, along with spots (which are crystallization features similar to lithophysae, but without a central cavity), can vary significantly in size, shape, abundance, and distance (or spacing) between features. In the Enhanced Characterization of the Repository Block (ECRB) Cross Drift, an inverse proportional relationship exists between the abundance of lithophysae and the number of fractures greater than 1 m in length (or the fracture frequency that is measured as the number of fractures per ten meters of tunnel) (Mongano et al. 1999). Using data from fractures with trace lengths greater than 1 m, the fracture system is typically characterized as "predominately" or "primarily" vertical (BSC 2004, Section 7.3.2);

however, these data also include shallowly dipping vapor-phase partings and randomly oriented fractures. The fabric of the lithophysal rock mass results from the integration of lithophysae (and spots) and fractures of various sizes, shapes, abundances, and spacings. It is the distribution and interaction (or lack of interaction) of these features on the scale of the drifts (about 10 m) that supports using a generally isotropic rock mass in the UDEC-Voronoi block model.

Lithostratigraphic features, including lithophysae, rims, spots, and fractures, are described in Appendix A and B of this response; however, many of the basic relations of these features that form the general fabric of the rock mass are summarized herein. The size, shape, abundance, and spatial distributions of features such as lithophysae and fractures control the failure mechanisms of the rock mass of the Tptpll. Lithophysae and similar features typically have diameters of 1 to 20 cm, but diameters of as much as 1.8 m have been measured. Typically, lithophysal cavities are roughly ovoid in shape with the long axis oriented approximately parallel to (and within ±20° of) the compaction foliation of the Tptpll. Distances between lithophysae can vary from centimeters to several meters. Fractures with trace lengths less than 1 m are similar to those with trace lengths greater than 1 m; however, the data also display increased variation in orientations such that there is much more randomness in the orientations of the smaller (less than 1 m) trace length fractures. Fractures in the Tptpll have a wide range in trace lengths, and the less than 1-m trace length data indicate a mean length of 0.281 m and a median length of 0.140 m. The fracture terminations indicate that about one third of the fractures "terminate in rock," thereby forming rock bridges, and most of the other terminations are in other fractures, and lithophysae. Many fractures are associated with lithostratigraphic features such as vapor-phase minerals, rims, borders, and color of adjacent matrix-groundmass that indicate many of the fractures and associated features formed during the period of time when the deposit was cooling. Together, the distributions of lithostratigraphic features such as lithophysae, spots, and fractures form a fabric of the rock in the Tptpll that has the potential to break into relatively small blocks. Comparison of nearby measurements (within 10 to 30 m) indicates similar types of variations in lithostratigraphic features, and at these lengths along the tunnel, the fabric of the rock can be represented as homogeneous. At longer lengths along the tunnel (such as 50 to 100 m), the ranges in abundance, size, separation distances, and orientations of features typically differ because of the stratiform (informal subzone) relations within the Tptpll.

Based on the lithophysal porosities, which were correlated with physical and mechanical properties, the lithophysal rocks in the Tptpll are divided into five rock property categories (BSC 2004, Figures 6-115, E-9, and E-10, and Table E-10; SAR Section 2.3.4.4.2.3.7, Figures 2.3.4-29 and 2.3.4-30). In the ECRB Cross Drift, the variations in the lithostratigraphic features locally and along the tunnel are consistent with using relatively homogeneous properties for the rock mass for local (drift-scale) conditions, and support the use of the five lithophysal and rock property categories. Use of the UDEC-Voronoi block model to approximate the characteristics of the lower lithophysal zone of the Topopah Spring Tuff (Tptpll) is based on: (1) lithophysae and fracture data from different scales of observation, and (2) how these data were abstracted for the choice of parameters in the UDEC model.

1.2 IMPACT OF FRACTURES AND LITHOPHYSAE ON ANISOTROPY

[NOTE: Zones of the Topopah Spring Tuff identified in this paragraph are as follows: Tptrn, crystal-rich nonlithophysal zone; Tptpul, upper lithophysal; Tptpmn, middle non-lithophysal; Tptpll, lower lithophysal; Tptpln, lower nonlithophysal.] Short-length fractures (less than 1-m trace length), coupled with the lithophysae, and are the most important features that govern stability of the rock mass in the Tptpll unit (BSC 2004, Sections 6.1.4.1 and E4). Abundant fractures are present throughout the Tptpll, with a lateral spacing of a few centimeters. Small-scale fracture traverses in the Tptpll confirm (see Section B1, second bullet, for description) the close spacing and short trace lengths of fractures in this zone (BSC 2004, Section 6.1.4.1). The close spacing and short trace lengths create a rock texture that limits the potential block size in this zone to be on the order of the spacing between pre-existing fractures and lithophysae. This is confirmed when large diameter core is removed from boreholes in the middle portion of the Tptpll (Figure A-11; BSC 2004, Figure 7-1a). The core, although competent, has numerous fractures that could break into small blocks when stressed. Thus, the lithophysae and occasional horizontal fractures tend to create blocks with dimensions of about 10 to 30 cm on a side. Thin section analyses of the fracturing in the Tptpll and the Tptpmn show rims on many of the fracture surfaces within the rock mass away from the tunnel wall, indicating there are numerous natural fractures that were formed during the cooling process (BSC 2004, p. 6-16). Analyses of slabs of core from surface-based and tunnel-based boreholes exhibit similar relations of rims and other features on fractures in the Tptrn, Tptpul, Tptpmn, Tptpll, and Tptpln that indicate natural fractures were formed throughout the rock mass during the cooling history of the Topopah Spring Tuff (BSC 2005).

Although the fracture orientation is described as primarily vertical because this is the dominant feature that is observed visually (in addition to the lithophysal cavities), the pattern of fracture orientations is usually much more complex. For example, a section from the upper portion of the Tptpll shows intensive fracturing of the matrix-groundmass between lithophysae, several "circum-lithophysal" fractures (fractures that formed around or parallel to the margins of lithophysae), and a few fractures that actually intersect the lithophysae (BSC 2004, Figure 6-10b). As a second example, Figure A-10 in Appendix A shows a geologic map of slot 2/B in slot test #1 at Exploratory Studies Facility (ESF) station 57+77 in the Tptpll. The complexity of the rock fabric in the Tptpll unit, with irregularly shaped lithophysae shown in red and short-length fractures shown in black, is clearly evident in this map. As shown in the figure, the fractures in section view are characterized by: (1) being sinuous, not straight, (2) commonly having rapid changes in orientation at the scale of 5 to 15 cm, and (3) being quite rough, not planar, at a scale of several centimeters. These three aspects govern the formation of blocks and give the blocks the complex surface characteristics that lead to the tunnel wall stability when seismically loaded.

Under thermal or seismic loading, stress concentrations can occur at or near the lithophysal voids. For example, a circular hole in a strained plate can amplify the uniform stress applied at the ends of the plate by a factor of 3 (Timoshenko et al. 1970, Chapter 4, Section 35). The presence of lithophysae in the Tptpll unit will function in a similar fashion, providing locations for stress concentrations under external loads and leading to preferential failure of the rock matrix between the randomly located lithophysae, rather than through displacement of small

blocks on short-length fractures. This failure pattern is also seen in numerical simulations of lithophysal rock mass compression documented in *Peak Ground Velocities for Seismic Events at Yucca Mountain* (BSC 2005, Appendix A, Section A1.1.3, and Appendix B, Section B2.1). The random locations and shapes of the lithophysae (e.g., Appendix A, Figure A-10) and the close spacing and short trace lengths of fractures indicate that a homogeneous, isotropic model provides a reasonable representation for modeling mechanical response in the Tptpll unit because the size of the internal structure and spacing of fractures is much smaller than the size of a drift, approximately 5.5 m in diameter.

1.3 EFFECT OF POTENTIAL ANISOTROPY ON DRIFT STABILITY

Drift stability is based on: (1) the geologic conditions in the upper half of a tunnel (from springline to crown to springline), and (2) the types of induced stress. While some anisotropy exists at various scales in the rock mass, the anisotropy does not significantly affect damage and fracturing in the drift crown where the major principal stress and stress-induced fractures are normal to the subvertical fractures. The largest thermally induced stresses and potential damage caused by those stresses would occur in the drift crown. Thus, anisotropy, if it exists, would not affect the drift stability or the model prediction of drift degradation during the thermal cycle. The springlines, in the ESF and ECRB Cross Drift, could be affected by possible anisotropy due to vertical fracturing. Yet the springlines are stable without any support, more than 10 years after excavation.

The 11.5-inch-diameter samples of Tptpll illustrated in Figure 1 were taken from the horizontal boreholes drilled in the drift springline. They were tested by applying the load in the direction aligned with the core axis, which corresponds to the horizontal *in situ* direction (i.e., perpendicular to the subvertical fractures). The maximum thermally induced stresses would be horizontal in the drift crown (Figure 1), and in the same direction in which the samples were tested. The six test results on the samples taken in the Tptpll (BSC 2004, Table E-9) are generally in good agreement with, or even exceed, the strength compared to the mean curve of the strength versus stiffness relation (BSC 2004, Figure E-13) for the lithophysal tuff. Thus, the Voronoi block model that is calibrated to five rock mass categories corresponding to equally spaced points on the mean curve (BSC 2004, Figure E-13) adequately represents conditions of deformation and damage in the drift crown where the peak thermal stresses will be experienced.

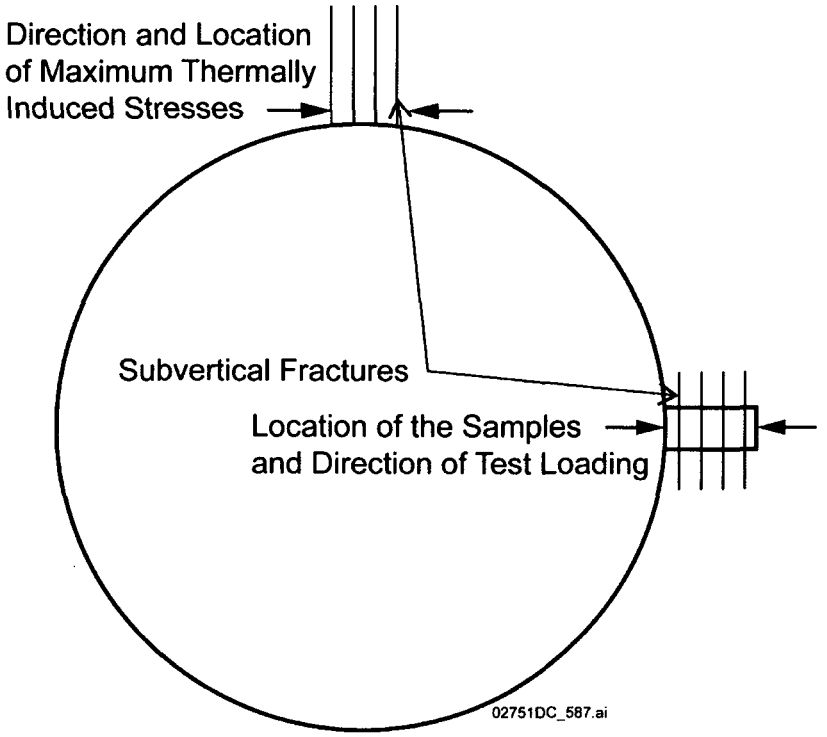

NOTE: For illustrative purposes.

Figure 1. Illustration of the Location of the Tested Samples and Testing Direction Compared with Location and Direction of the Maximum Induced Thermal Stresses

Breakouts around tunnels excavated in overstressed rocks form as a result of coalescing of fractures parallel and subparallel to the tunnel wall at the location of the stress concentration. An example of such fractures, which did not result in breakout in this particular case, is observed in the boreholes drilled in the drift springline in the poor quality (Category 1) Tptpll as shown in the upper left corner of Figure 2. The figure also illustrates that the UDEC Voronoi block model realistically represents the mechanism of fracturing parallel to the drift wall.

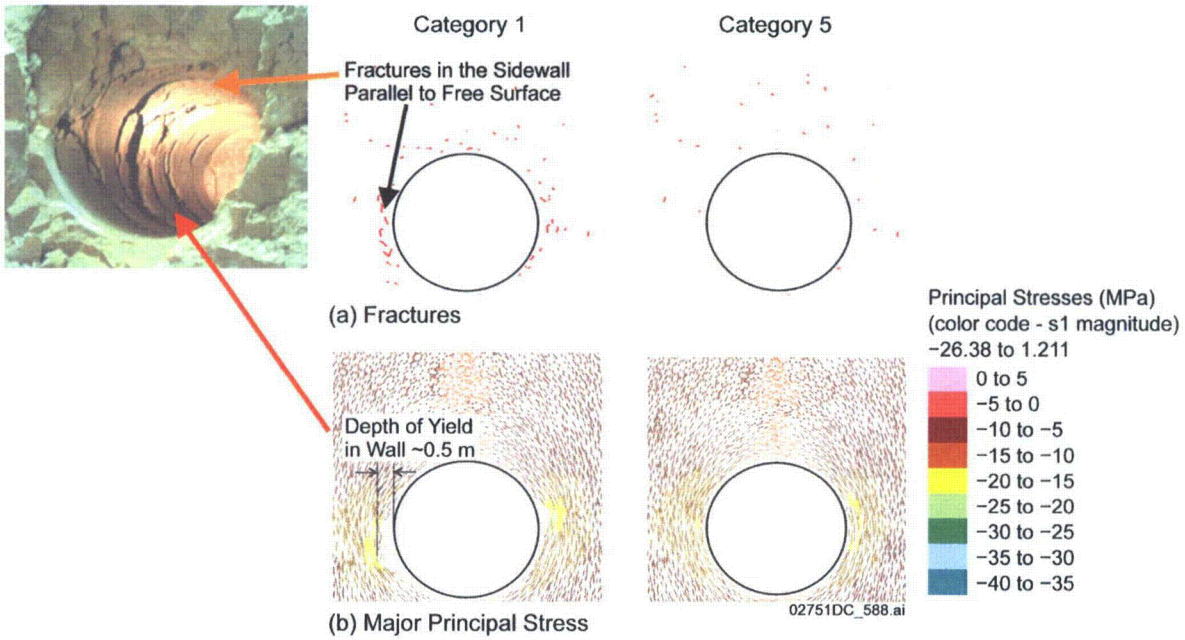

Source: BSC 2004, Figure 7-26.

NOTE: Upper figure (a) for Category 1 shows predicted fracturing to a depth of approximately 0.5 m in the sidewall of the ECRB Cross Drift. Lower figure (b) shows stress vectors (in Pa) colored by the magnitude of the stress component. Depth of yield for Category 1 is limited to about 0.5 m in the immediate springline area. The model for Category 5 (a) shows elastic rock mass response (i.e., no yield). Stress vectors in lower figure (b) also show elastic stress distributions with no readjustment due to yielding.

Figure 2. Observed Wall Parallel Fractures in a 12-Inch-Diameter Horizontal Borehole Drilled in the Springline of the ESF in Low Quality Tptpll (approximately Category 1) and Its Representation in the UDEC Voronoi Block Model

The reason for this kind of failure mechanism is that the stress state in the drift wall is approximately the same as the unconfined compression, in which the major principal stress is parallel to the drift wall while confinement normal to the drift wall is zero. Lithophysal tuff and similar rocks fail under unconfined conditions by axial splitting in which the cracks propagate in the direction of the major principal stress (i.e., the loading direction). Axial splitting as observed in a laboratory experiment and simulated with the Voronoi block model is shown in Figure 3.

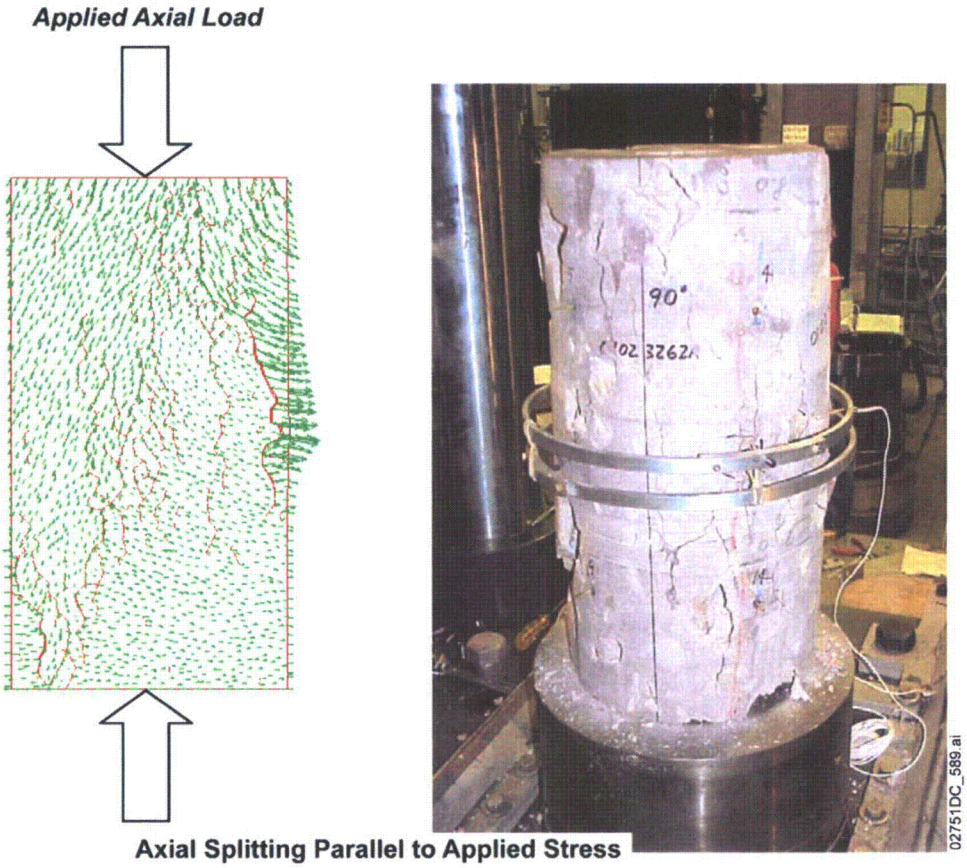

Source: BSC 2004, Figure 7-23.

NOTE: The model predicts axial splitting when no confinement is applied as seen by the red tensile block boundary breakages (fractures) formed and by the velocity vectors that show the sidewall spalling. Core photo shows similar axial splitting phenomena.

Figure 3. UDEC Discontinuum Model of Failure of Lithophysal Tuff Specimen under Uniaxial Compression

Thus, if there is an effect of anisotropy in the fracturing in the Tptpll (i.e., predominantly vertical fractures) on damage around the emplacement drifts, it would be evident in the drift wall in the springline, where subvertical fractures are parallel to the orientation of the major principal stress and to the orientation of the stress-induced fractures. Anisotropy, as manifest as fracture patterns in the tunnels, is visually apparent, but has no effect on damage and fracturing in the drift crown where the major principal stress and stress-induced fractures are normal to the subvertical fractures. The largest thermally induced stresses and potential damage caused by those stresses will be in the drift crown. Thus, if anisotropy affects the mechanical response, it would not affect the drift stability or the model prediction of drift degradation during the thermal cycle. On the other hand, the drift springline in the ESF and ECRB Cross Drift, which would be affected by possible anisotropy due to vertical fracturing, is stable without any ground support, more than 10 years after excavation. Boreholes (e.g., Figure 1) in poor quality lithophysal rock show evidence of fracturing that did not cause any drift instability.

Sources (e.g., Jaeger and Cook 1979, Section 4.10) discuss the effect of anisotropy on strength of rocks, which is based on consideration of slip on ubiquitous continuous planes (e.g., bedding planes). However, those effects analyses are not applicable to the emplacement drift stability because fractures in the lower lithophysal tuff are not continuous with infinite length. Instead, they have finite length with rock bridges or intact rock between them that prevent slip.

1.4 VALIDATION OF OBSERVATIONS

The representation of rock mass stress and yield characteristics around drifts is confirmed by the validation of the drift-scale modeling of lithophysal rock with the UDEC program (BSC 2004, Section 7.6). The UDEC model for lithophysal rock is based on randomly oriented contacts (boundaries) between adjacent rock blocks, resulting in isotropic response at the scale of a drift. The UDEC validation is based on comparison of UDEC results with:

1. Observations of failure mechanisms in the laboratory
2. Field observations of tunnel response in the ECRB Cross Drift
3. Thermally induced fracture development in the Drift Scale Test within the Tptpmn unit
4. Literature data from related field experiments in which blast-induced yield of a jointed rock mass and large deformations of a scaled, lined tunnel are induced
5. Comparison of the output predictions of rock mass stress and yield around emplacement drifts using the UDEC discontinuum model of lithophysal rock to alternative continuum-based representations of the mechanical response of lithophysal rock.

Items 1 to 3 and 5 are information about conditions specific to Yucca Mountain. Comparisons for items 1 to 3 confirm that the isotropic model in UDEC provides a reasonable representation of Tptpll response at the drift scale.

1.5 SUMMARY

The random locations and shapes of the lithophysae and the close spacing and short trace lengths of fractures are characteristic of the Tptpll. These characteristics are consistent with the use of a homogeneous, isotropic model to reasonably represent the mechanical response of the Tptpll unit. The close spacing and short trace lengths create a rock texture that limits the potential block size in this zone to be on the order of the spacing between pre-existing fractures and lithophysae (~10 to 30 cm). In addition, the presence of lithophysae in the Tptpll unit function in a similar fashion, providing locations for stress concentrations under external loads and leading to preferential failure of the rock matrix between the randomly located lithophysae.

Visually apparent anisotropy does not affect damage and fracturing mechanics of the drift crown where the major principal stress and stress-induced fractures are normal to the subvertical fractures. The largest thermally induced stresses and potential damage caused by those stresses would occur in the drift crown. Thus, if anisotropy exists, it would not affect the drift stability or the model prediction of drift degradation during the thermal cycle. The drift springline in the

ESF and ECRB Cross Drift could be affected by possible anisotropy due to vertical fracturing. Yet the springlines are stable without any ground support, more than 10 years after excavation, indicating that any anisotropy present in the walls is not mechanically significant.

This response provides descriptions of the rock mass texture and additional technical bases for representing the Topopah Spring Tuff lower lithophysal unit as homogeneous at the scale of the drifts (approximately 5.5m). Based on the analyses summarized above, the Voronoi block model uses an appropriate representation of the characteristics of the Topopah Spring Tuff lower lithophysal unit, and the potential for drift collapse has not been underestimated by the model.

2. COMMITMENTS TO NRC

None.

3. DESCRIPTION OF PROPOSED LA CHANGE

None.

4. REFERENCES

BSC (Bechtel SAIC Company) 2004. *Drift Degradation Analysis.* ANL-EBS-MD-000027 REV 03. Las Vegas, Nevada: Bechtel SAIC Company. ACC: DOC.20040915.0010; DOC.20050419.0001.

BSC 2005. *Peak Ground Velocities for Seismic Events at Yucca Mountain, Nevada.* ANL-MGR-GS-000004 REV 00. Las Vegas, Nevada: Bechtel SAIC Company. ACC: DOC.20050223.0002; DOC.20050725.0002.

BSC 2007. *Subsurface Geotechnical Parameters Report.* ANL-SSD-GE-000001 REV 00. Las Vegas, Nevada: Bechtel SAIC Company. ACC: ENG.20070115.0006.

Buesch, D.C.; Spengler, R.W.; Moyer, T.C.; and Geslin, J.K. 1996. *Proposed Stratigraphic Nomenclature and Macroscopic Identification of Lithostratigraphic Units of the Paintbrush Group Exposed at Yucca Mountain, Nevada.* Open-File Report 94-469. Denver, Colorado: U.S. Geological Survey. ACC: MOL.19970205.0061.

Buesch, D.C. and Spengler, R.W. 1998. "Character of the Middle Nonlithophysal Zone of the Topopah Spring Tuff at Yucca Mountain." *High-Level Radioactive Waste Management, Proceedings of the Eighth International Conference, Las Vegas, Nevada, May 11-14, 1998.* Pages 16-23. La Grange Park, Illinois: American Nuclear Society.

FRACMAN V. 2.512. 1999. WINDOWS NT.

Jaeger, J.C. and Cook, N.G.W. 1979. *Fundamentals of Rock Mechanics.* 3rd Edition. New York, New York: Chapman and Hall.

Mongano, G.S.; Singleton, W.L.; Moyer, T.C.; Beason, S.C.; Eatman, G.L.W.; Albin, A.L.; and Lung, R.C. 1999. *Geology of the ECRB Cross Drift - Exploratory Studies Facility, Yucca Mountain Project, Yucca Mountain, Nevada.* Deliverable SPG42GM3. Denver, Colorado: U.S. Geological Survey. ACC: MOL.20000324.0614.[a]

Otto, S.J. and Buesch, D.C. 2003. "Porosity, Bulk Density, and Rock-Particle Density of Lithostratigraphic Components in Lithophysal Rocks of the Topopah Spring Tuff at Yucca Mountain, Nevada." Abstracts with Programs - Geological Society of America, 35, (6), 434-435. Boulder, Colorado: Geological Society of America.

Smart, K.J.; Wyrick, D.Y.; Landis, P.S.; and Waiting, D.J. 2006. *Summary and Analysis of Subsurface Fracture Data from the Topopah Spring Tuff Upper Lithophysal, Middle Nonlithophysal, Lower Lithophysal, and Lower Nonlithophysal Zones at Yucca Mountain, Nevada.* CNWRA 2005-04. San Antonio, Texas: Center for Nuclear Waste Regulatory Analyses. ACC: MOL.20070917.0439.

SNL (Sandia National Laboratories) 2008. *Technical Report: Geotechnical Data for a Geologic Repository at Yucca Mountain, Nevada.* TDR-MGR-GE-000010 REV 00. Las Vegas, Nevada: Sandia National Laboratories. ACC: DOC.20080206.0001.

Timoshenko, S.P. and J.N. Goodier, 1970. *Theory of Elasticity.* Third Edition. McGraw-Hill Book Company, New York, New York.

UDEC V. 3.14. 2004. WINDOWS 2000.

NOTE: [a]Provided as an enclosure to letter from Williams to Jacobs, dtd 9/24/2009, Yucca Mountain - Supplemental Responses to Requests for Additional Information (RAI) - Volume 2, Chapter 2.1.1.1, First Set and Second Set - Site Description

5. LIST OF ATTACHMENTS

APPENDIX A: LITHOPHYSAL DATA [Note: The information provided in Appendix A has been summarized from *Drift Degradation Analysis* (BSC 2004, Appendix O).]

APPENDIX B: FRACTURE DATA [Note: The information provided in Appendix B has been summarized from *Drift Degradation Analysis* (BSC 2004, Appendix B).]

APPENDIX A
LITHOPHYSAL DATA

The lithophysal data are divided into primary input data and supporting data, which are described separately below. Because of the configuration of the ESF and ECRB Cross Drift, most of the data for the Tptpll are from the ECRB Cross Drift; however, some data are from the ESF and others are from surface-based boreholes. In relation to the shallowly dipping lithostratigraphic section at Yucca Mountain, including the Tptpll, the configuration of the ECRB Cross Drift results in a full lithostratigraphic section of the Tptpll being exposed in the ECRB Cross Drift (distributed along 882 m of tunnel).

Geologic studies document one- and two-dimensional distributions of lithostratigraphic features such as lithophysae, rims, spots, lithic clasts, and the matrix-groundmass. A lithophysa consists of a central cavity that is typically lined with vapor-phase minerals, and the cavity is surrounded by a rim. Rims and spots are crystallization features with similar mineralogy (feldspar and quartz or cristobalite) and textures (such as fine-grained spherulites and porosity that ranges from 20% to 40%; Otto and Buesch 2003). Rims form on lithophysal cavities and along the margins of some fractures, and spots are similar to lithophysae, but without a central cavity. The matrix-groundmass typically displays the vitroclastic textures of pyroclastic flow deposits; however, the glass that was part of the original deposit has crystallized to fine-grained feldspar and quartz (or cristobalite), and typically, the porosity of the matrix-groundmass in the Tptpll is about 10.4% (Otto and Buesch 2003). In some data collection and description of rocks, rims and spots are described separately from the matrix-groundmass; however, in other descriptions, the rims, spots, and matrix-groundmass are included as "rock" or "matrix." The most used and cited data are summarized and developed in *Drift Degradation Analysis* (BSC 2004); other reports such as *Subsurface Geotechnical Parameters Report* (BSC 2007), and *Peak Ground Velocities for Seismic Events at Yucca Mountain, Nevada* (BSC 2005) also provide data on these lithostratigraphic features. In *Drift Degradation Analysis* (BSC 2004), most of the analysis of lithophysal and porosity data focused on the development of estimates of the total abundance of lithophysae (or porosity) at specific locations along the ECRB Cross Drift.

A1 PRIMARY LITHOPHYSAL INPUT DATA FROM PANEL MAPS AND ANGULAR TRAVERSES

Primary lithophysal input data are from observations made in the ECRB Cross Drift, which include tape traverses, angular traverses, panel maps, and large-lithophysae inventory data, and these are summarized and developed in *Drift Degradation Analysis* (BSC 2004, Appendix O). The tape traverse data were collected along a line traverse across the upper part of the tunnel (for most traverses this was in the upper two thirds of the tunnel profile), and the traverses were made every 5 m along the tunnel. Because only lithophysal cavity data were collected along the traverse, these data are one-dimensional discontinuous data. There are 22 angular traverses that were collocated with tape traverses; however, the angular traverses measured the positions and intercept distances for all features (lithophysal cavities, rims, spots, lithic clasts, and the matrix-groundmass). Because data on all features were collected along the traverse, these data are one-dimensional continuous data. The 18 panel maps are 1 × 3 m and depict the side wall (or rib) of the tunnel where the wall is effectively vertical (near spring line), showing all features.

Because data on all features were collected in the panel area, these data are two-dimensional continuous data. The large-lithophysae inventory documented lithophysae with a minimum diameter of 50 cm located anywhere along the tunnel walls. Because only lithophysal cavity data were collected along the tunnel wall, which can be treated as a cylindrically folded plane, these data are two-dimensional discontinuous data. All four types of data are described individually, and they are combined to produce estimates of abundances of lithophysal cavities, rims, spots, lithic clasts, and the matrix-groundmass both locally and along the tunnel.

There are seven relations of lithophysae, which represent local and along-the-tunnel variations, that support the depiction of the rock mass as locally and generally isotropic:

- Each tape and angular traverse, each panel map, and the large-lithophysae inventory data as a whole contain a range (and some have a wide range) in amounts and sizes of lithophysae. Additionally, the angular traverse and panel data include amounts and sizes of rims, spots, and lithic clasts.

- About 77% of the intercept lengths in the tape traverse data are less than 20 cm, and 98% have intercept lengths less than 50 cm (BSC 2004, Figure O-19). It is important to remember that linear traverse data such as in a tape or angular traverse only represent the intercepted length across a feature (and typically the intercepted length is less than the diameter); therefore, these data provide a general representation of the size distributions of lithophysal cavities. These values are consistent with most lithophysal cavities having a variety of sizes, of which most are less than 20 cm. These data also indicate why the tape traverse data and large-lithophysae inventory represent complementary data.

- Variations in the total adjusted trace lengths of lithophysal cavities, both locally and along the tunnel, are represented by the variance calculated for each tape traverse (BSC 2004, Figure O-20). Again, as mentioned in the point above, linear traverse data such as the tape traverse data are helpful for examining trends in data, and each traverse represents only a narrow sampling of a two- or three-dimensional object; therefore, the amount of variation can be large from one location to the next. Thus, the 5-m data indicate local variations, and the moving average data help define lateral trends (and in the Tptpll in the ECRB Cross Drift, this is equivalent to lithostratigraphic position in the zone).

- The large-lithophysae inventory data indicate overall variations in position, size, and abundance locally; however, there are trends in these values that are consistent with stratigraphic position within the Tptpll (BSC 2004, Figure O-12).

- The variations along the tunnel in the abundance of lithophysal cavities and the large-lithophysae inventory data (and other lithostratigraphic data) conceptually support identification of subzones in the Tptpll.

- The porosity along the tunnel of the lithophysal cavities, rims and spots, matrix-groundmass, and the total porosity was calculated from layering and adjusting the four types of data. The along-the-tunnel porosity profiles were determined with slightly

different data and presented as Figures O-15 and O-16 in *Drift Degradation Analysis* (BSC 2004). Figure O-16 from that report (BSC 2004) is included in this response as Figure A-1.

- Two-dimensional simulations of the lithophysal cavity porosity in the Tptpll are presented in Figure T-5 of *Drift Degradation Analysis* (BSC 2004). Figure T-5 is included in this response as Figure A-2. These simulations are vertical cross sections perpendicular to the ECRB Cross Drift and (1) they are based on the data from the ECRB Cross Drift, and (2) they are consistent with the lateral continuity of lithostratigraphic units (that is, stratiform characteristics) that have been demonstrated in other lithostratigraphic studies (Buesch et al. 1996). These simulations are statistically identical to the along-the-tunnel porosity data as projected onto the vertical plane. Although the values were not adjusted based on nearest neighbor comparisons (meaning they were not adjusted to diminish or smooth sharp differences in values in adjacent cells), on the near-drift scale of 5 to 10 m, these simulations indicate a relatively homogeneous porosity at any given point on the section. These spatial variations in porosity were used to simulate variability in properties in the UDEC Voronoi model simulations (BSC 2004, Figure E-15).

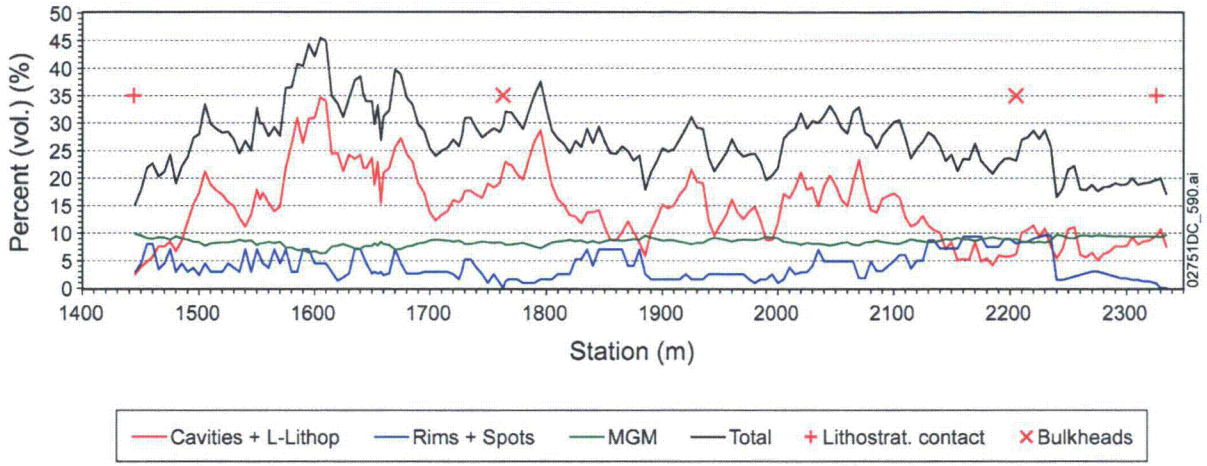

Source: BSC 2004, Figure O-16.

Figure A-1. Calculated Porosity of Lithophysal Cavities (including large lithophysae), the Combination of Rims and Spots, Matrix-Groundmass (MGM), and the Total Porosity in the Tptpll Exposed in the ECRB Cross Drift from Station 14+44 to 23+30

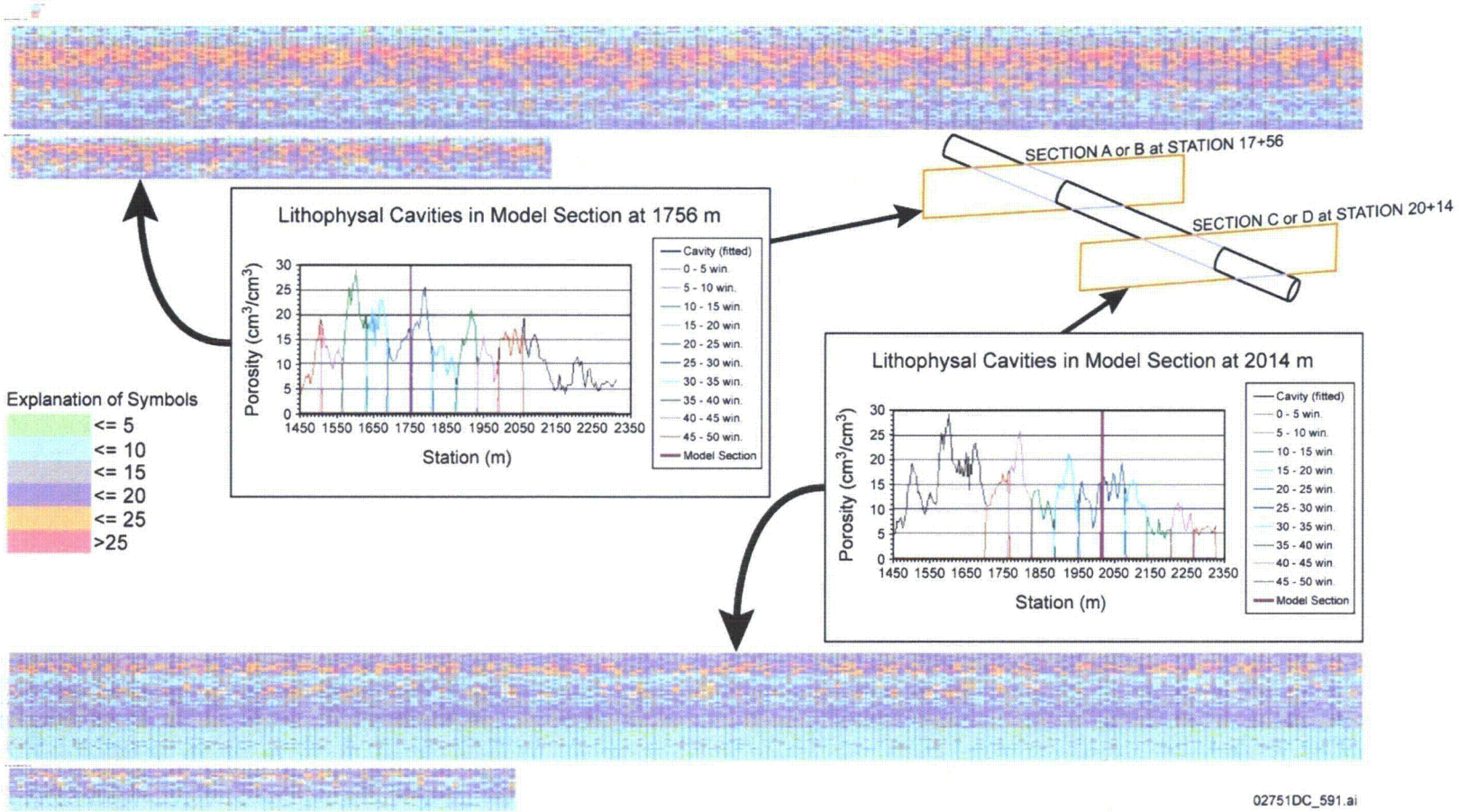

Source: BSC 2004, Figure T-5.

NOTE: Cross section A is a 50 × 200 cell table representing a 1 × 1 m grid, and cross section B is a 20 × 80 cell table representing a 2.5 × 2.5 m grid for the simulated section at 17+56. Cross Section C is a 50 × 200 cell table representing a 1 × 1 m grid, and cross Section D is a 20 × 80 cell table representing a 2.5 × 2.5 m grid for the simulated section at 20+14. The lower parts of Sections A and B are similar to the upper parts of Sections C and D; this results from an overlap in the sampled data from along the tunnel.

Figure A-2. Two 50 × 200 m Simulated Cross Sections of Lithophysal Cavity Porosity at Stations 17+56 and 20+14

A2 SUPPORTING LITHOPHYSAL DATA

There are five sources of supporting lithophysal data: (1) additional details in the data package for lithophysal studies in the ECRB Cross Drift, (2) distributions of lithophysae identified in photographs of tunnel walls in the ECRB Cross Drift, (3) data from video analysis of borehole USW WT-2, (4) data supporting the Thermal Conductivity Tests (Therm-K-series boreholes) and Slot Tests, and (5) photographs of core. Typically these data are from detailed investigations in the tunnels, boreholes, and in core. These data provide details on size, abundance, and spatial distribution (distance between and orientation) of local features. Typically these details are challenging to incorporate into local or larger-scale numerical models; therefore, these data provide conceptual and qualitative (if not semi-quantitative) context in the development of models.

A2.1 Lithostratigraphic Features in Angular Traverse and Panel Map Data

Most of the supporting lithophysal data are from the lithophysal studies in the ECRB Cross Drift, and these data include: (1) measurements of specific features (including lithophysae) such as size or traverse intercept length, (2) distance between features whether specifically measured, or simply documented on the panel maps, and (3) the orientation (apparent dip) of the long axis of lithophysae in panel maps. Typically, only the total amounts of features in each of the traverses and panel maps were used in the calculations for the porosity along the tunnel; however, these traverses and panel maps indicate local variations in size, shape, and abundance of the features.

Examples of angular traverse and panel map data:

- Angular traverse data document the positions and lengths along the traverse of lithostratigraphic features, including lithophysal cavities, rims, spots, and lithic clasts (Figures A-3 and A-4).

- Panel maps document the positions and areas lithostratigraphic features, including lithophysal cavities, rims, spots, and lithic clasts (Figures A-5 and A-6).

- Panel maps and the large-lithophysal inventory, and in part the angular traverse data, document the qualitative and semi-quantitative shapes of lithophysae, spots, and lithic clasts. Qualitative shapes are based on visual inspection and include simple (S); merged (M); cuspidate (C), and expansion-crack (E). The relative abundances of these data are summarized in *Peak Ground Velocities for Seismic Events at Yucca Mountain, Nevada* (BSC 2005, Section A1.1.2, Table A1-5). Panel maps and the large-lithophysal inventory document semi-quantitative shapes based on measured lengths of the apparent long and short axes of the feature that are exposed on the tunnel wall, and these values are used to calculate the aspect ratio (that is, the long axis divided by the short axis). Additionally, the panel maps include measured depths into the wall and a qualitative shape of the cavity. In the large-lithophysae inventory, the positions of lithophysae on the tunnel wall are simplified into eight positions with positions 2 and 6 on the left and right walls, respectively (BSC 2004, Figure O-12). For large-lithophysae along the left and right walls, the range in aspect ratios is 1.00 to 4.33, with mean ratios of 1.48 and 1.55 for the

left and right walls (respectively) and standard deviations of 0.50 and 0.60 (respectively). With the greater detail of all sizes of lithophysae in the panel maps, which were positions along the left and right walls, the range in aspect ratios is 1.00 to 110.00 (for both walls) with a mean ratio of 4.33 and a standard deviation of 7.82. These data indicate that the larger lithophysae tend to be closer to circular in cross section whereas smaller lithophysae (those less than about 0.5 m in diameter) can also be nearly circular in cross section; however, many are more elliptical in cross section (and some are very elongate).

- Panel maps document the generally subhorizontal orientation of lithophysal cavities, which is similar to (within ±20°) the compaction foliation of the Topopah Spring Tuff. Most of the panel maps are in the segment of the ECRB Cross Drift that has an azimuth of 229°; therefore, apparent dips in the wall of the tunnel that are toward the heading would be to the southwest, and those away from the heading would be to the northeast. The angles of apparent dips were measured for all lithophysae; however, explicit directions were recorded in about one-third of the panel maps. Where the directions were recorded, lithophysal axes typically dip as much as 15° (with some as much as 85°) to the southwest (toward the heading); however, most dip from 0° to 35° (with some as much as 90°) to the northeast.

A2.2 Lithophysae in Panel Photographs of Tunnel Walls along the ECRB Cross Drift

As part of *Peak Ground Velocities for Seismic Events at Yucca Mountain, Nevada* (BSC 2005), the distributions of lithophysae were compiled from various sources of data, including interpretations of panel photographs of tunnel walls along the ECRB Cross Drift (BSC 2005, Appendix A, Sections A1.1.2 and A4). Examples of panel photographs and maps from that report (BSC 2005) include Figures A1-17, A1-19, and A4-1 to A4-12, with Figures A4-8 to A4-9 and A4-10b specifically from the Tptpll, and two of these examples are reproduced in this response as Figures A-8 and B-2. The lithophysae identified on the panel photographs were intended to augment the data previously collected in the panel maps; therefore, on panel photographs that contain a panel map, the individual lithophysae in the panel map typically were not depicted.

Summary of general relations of lithophysae from the panel photographs:

- The shapes and sizes of lithophysae are summarized in Figure A-7 (from Figure A1-17 in BSC 2005).

- Distances between lithophysae and spots can be measured from the panel photographs.

- Examples of panel photographs with lithophysae greater than 20-cm diameter are in Figure A-8 (from Figures A4-8 and A4-9 in BSC 2005).

A2.3 Borehole USW WT-2

Borehole USW WT-2 is located in the central block of Yucca Mountain and just east of the southern part of the proposed repository; therefore, this borehole provides data on lithophysae that are independent of data collected in the ESF and ECRB Cross Drift. The distributions and abundances of lithophysal cavities are from analysis of borehole video in USW WT-2. These data were collected to evaluate the relief (or rugosity) of borehole walls based on the occurrence of lithophysal cavities. Lithophysal cavities were counted (point counted) along two line traverses (one along the north wall and one along the east wall) in the segment of borehole that penetrated the upper lithophysal, middle nonlithophysal, lower lithophysal, and lower nonlithophysal zones of the Topopah Spring Tuff (Tptpul, Tptpmn, Tptpll, and Tptpln, respectively). Lithophysae were individually measured, and those that were large enough to be intercepted by both traverses were identified and labeled as "big" lithophysae. There are several segments of the borehole where breakouts occur, especially two very large breakouts (apparently along fractures) in the Tptpmn. The point count data document the transect length along the borehole wall of lithophysae, and a synthetic caliper was calculated based on the assumption that the transect length along the borehole is the same as the penetration depth into the wall. The lithophysae data and synthetic caliper for the north traverse are displayed in Figure A-9.

Summary observations from borehole USW WT-2:

- The abundance and size of lithophysae relative to the lithophysal and nonlithophysal zones are consistent with lithostratigraphic data elsewhere at Yucca Mountain.

- Because the synthetic caliper was developed from the occurrences of lithophysal cavities, and qualitatively there are good comparisons of the synthetic caliper values and caliper data measured in geophysical logs, it appears that most of the variations in the caliper logs probably result from lithophysal cavities or minor breakouts near or between the cavities.

- The lithophysal size and abundance data in borehole USW WT-2 are from a surface-based borehole (which is effectively vertical), so the variations in lithophysae are consistent with the stratigraphic position within each of the lithostratigraphic units (and there are hints of subzones). In contrast, the lithophysal data from the ECRB Cross Drift were collected along a subhorizontal tunnel through a shallowly dipping lithostratigraphic section; however, the section through the tunnel represents the complete section such as in the Tptpll. The USW WT-2 data, especially in the Tptpll, are consistent with the lithophysal data from the ECRB Cross Drift (and the hints of subzones).

- In the Tptpll of USW WT-2, the size, abundance, and spacing of lithophysae vary locally; however, if 15- to 30-ft-long segments are evaluated (similar to the 5- to 10-m segments in the ECRB Cross Drift and drift-scale models), then a local rendition of homogeneity is imposed on the overall stratigraphic variation through the zone.

A2.4 Thermal Conductivity Tests and Slot Tests

Some of the supporting lithophysal data are from data and maps based on analysis of borehole video recordings in the thermal conductivity tests (ThermK-series boreholes) and slot tests (Table A-1). Four thermal conductivity tests were conducted in the Tptpll (three in the ECRB Cross Drift and one in the ESF), and one was in the Tptpul in the ESF. The ThermK boreholes are small-diameter, horizontal boreholes, each of which is about 9 m long, and they were configured such that they intersect at 90°. Each borehole has a video recording. The abundances of lithostratigraphic features were determined using a calibrated grid overlay on a video recording image to determine the areas of features along 0.5-ft-long segments of the boreholes. Two slot tests were conducted in the Tptpll (one in the ECRB Cross Drift and one in the ESF), and one was in the Tptpul in the ESF. The configuration of the slot tests included a central 12-inch-diameter borehole between two slots. Borehole video recordings were collected for the borehole and slots. The position, size, and shape of lithostratigraphic features in the boreholes were determined and mapped using a calibrated grid overlay on the video recording image. The video recordings in the slots consisted of a series of "runs" into the slot, and each run was spaced vertically in 5-cm intervals such that there was some overlap in the field of view from one run to the next run. The position, size, and shape of lithostratigraphic features were determined and mapped using a calibrated grid overlay on the video recording image. A map was made for each run (and reconciled with the previous run) to ultimately produce a full map of the slot. It took 20 video runs to compile the geologic map for Slot 2/B in slot test #1 in the Tptpll at ESF station 57+77 (Figure A-10).

Summary observations from thermal conductivity tests and slot tests:

- The ThermK borehole data document the abundance (area) every 0.5 ft along the borehole of lithostratigraphic features, including lithophysal cavities, rims, and spots (and in a few boreholes, lithic clasts). The data also include counts of fractures in each 0.5-ft segment along the borehole. Individual lithophysae were not identified; however, they were divided into centimeter-sized and decimeter-sized lithophysae.

- Although the detailed borehole data are in essence three-dimensional data (that is the data are collected along the cylinder walls of a borehole), on the scale of each test (which is about 2 × 10 × 10 m), each borehole is basically linear traverse data. This configuration results in variability on the local scale; however, the abundance values were represented as averages for each test.

- Maps of the boreholes and slots in the three slot tests provide quantitative values for individual features and include summary statistics on the abundance and size distribution of features. Spatial distribution data are documented on the maps, although distances between objects were not specifically measured. Interactions of lithophysae, spots, and fractures are depicted on the maps, such as the map for Slot 2/B in slot test #1 in the Tptpll at ESF station 57+77 (Figure A-10). Some "plucking" of the walls during drilling might have enhanced the apparent apertures of some fractures and shapes of some

lithophysal cavities, but where possible, the boundaries of lithophysal cavities and some fractures were identified by the occurrence of rims or vapor-phase mineral coatings.

A2.5 Photographs of Core

Photographs taken of core provide local examples of lithostratigraphic features including lithophysae and fractures. Some photographs were taken as part of the documentation during field activities, including the recovery of core from boreholes of field relation of tests, whereas other photographs were taken to demonstrate specific features or relations. One example of a photograph of core is from borehole ECRB-GTEC-1928-01 in the Tptpll from the ECRB Cross Drift (Figure A-11). In the piece of core, lithophysae are identified by the cavity and the white vapor-phase mineral lining, the rims on lithophysae and spots are dark because they have retained water (from drilling) in the pore space, and fractures with various orientation and trace lengths are also identified because of water retained in the apertures or in rims along the fracture margins. The lithophysae in this piece of core are oblate (that is, the long axis approximates the compaction foliation of the rock), and the cavities have high aspect ratios (that is, the ratio or value obtained by dividing the length of the long axis by the length of the short axis).

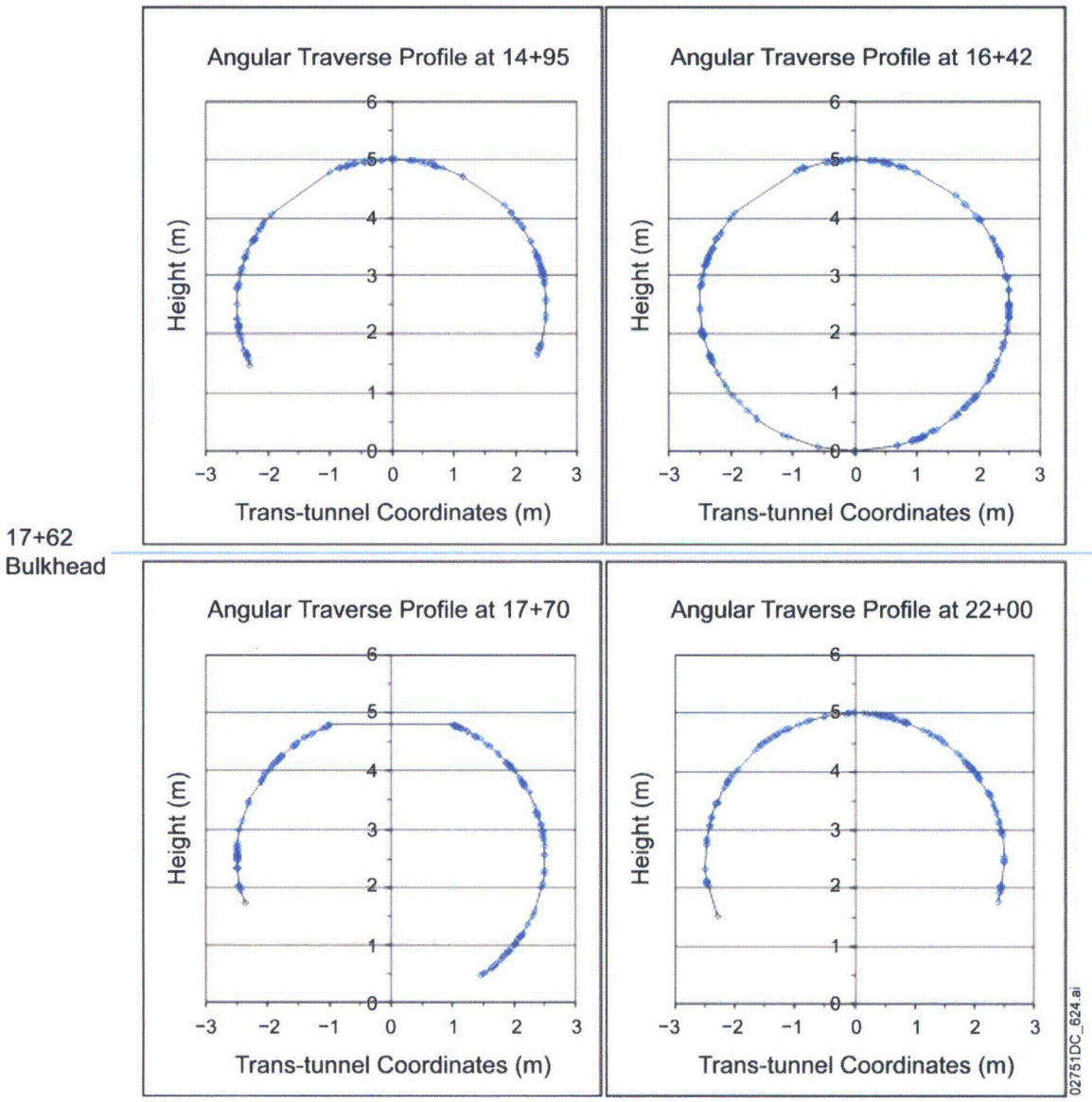

NOTES: There are two vent lines on both sides of the crown (top of the tunnel) for profiles at 14+95 and 16+42, one vent line for the profile at 17+70, and no vent line at profile 22+00.

Diamonds are the beginning and ending of a feature, including lithophysal cavities, rims, spots, and equipment such as vent lines or pipes.

Figure A-3. Locations of Lithophysal Cavities, Rims, Spots, and Lithic Clasts in Four Angular Traverses in the Tptpll of the ECRB Cross Drift

NOTE: Symbols are plotted at the beginning of the feature as the traverse angles decrease from 300° to 30°.

Figure A-4. Positions along the Traverse and Lengths of Lithostratigraphic Features in Angular Traverse 14+60

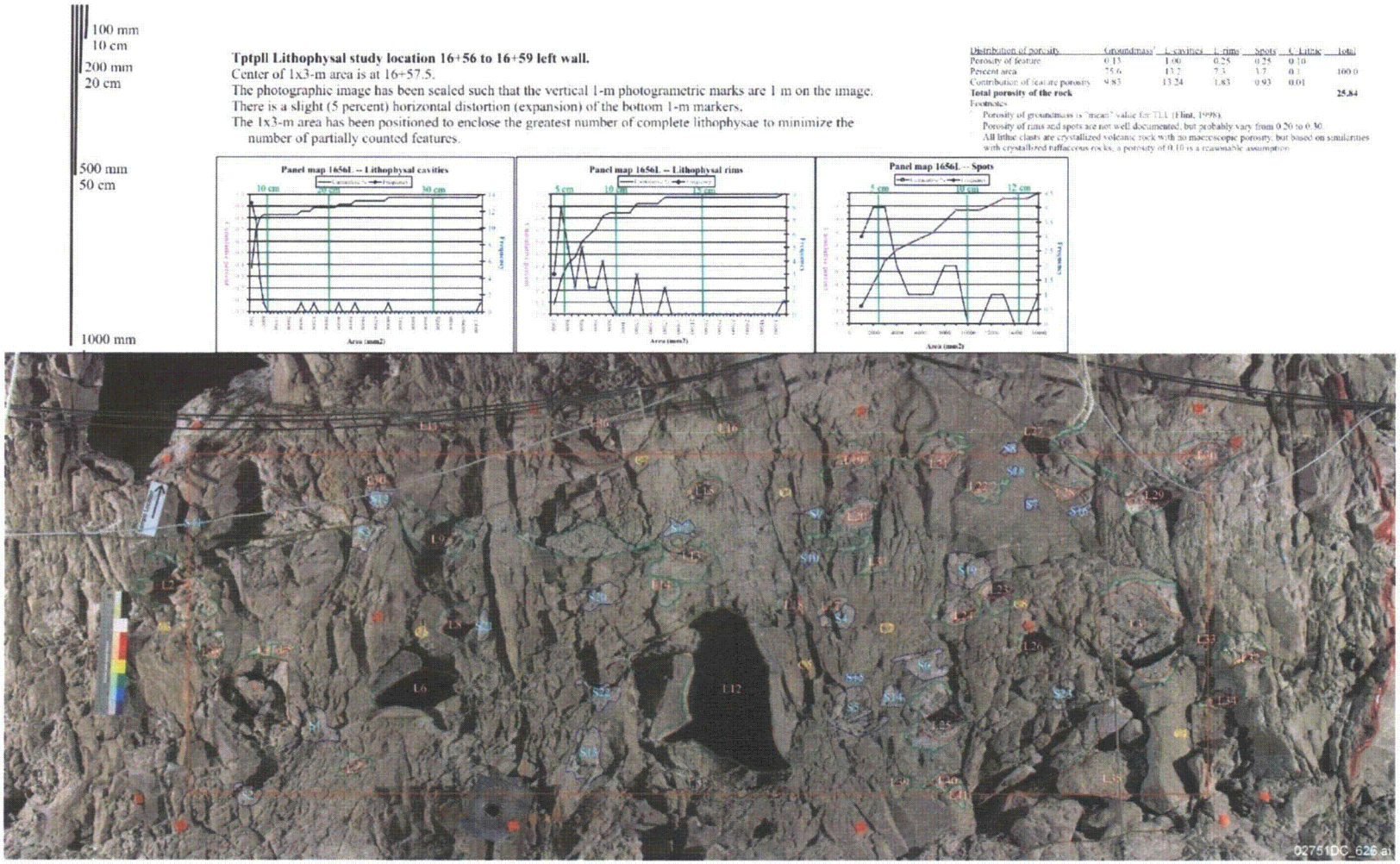

Source: BSC 2005, Figure A3-7.

Figure A-5. Positions and Sizes of Lithostratigraphic Features in Panel Map at 16+56 (left wall)

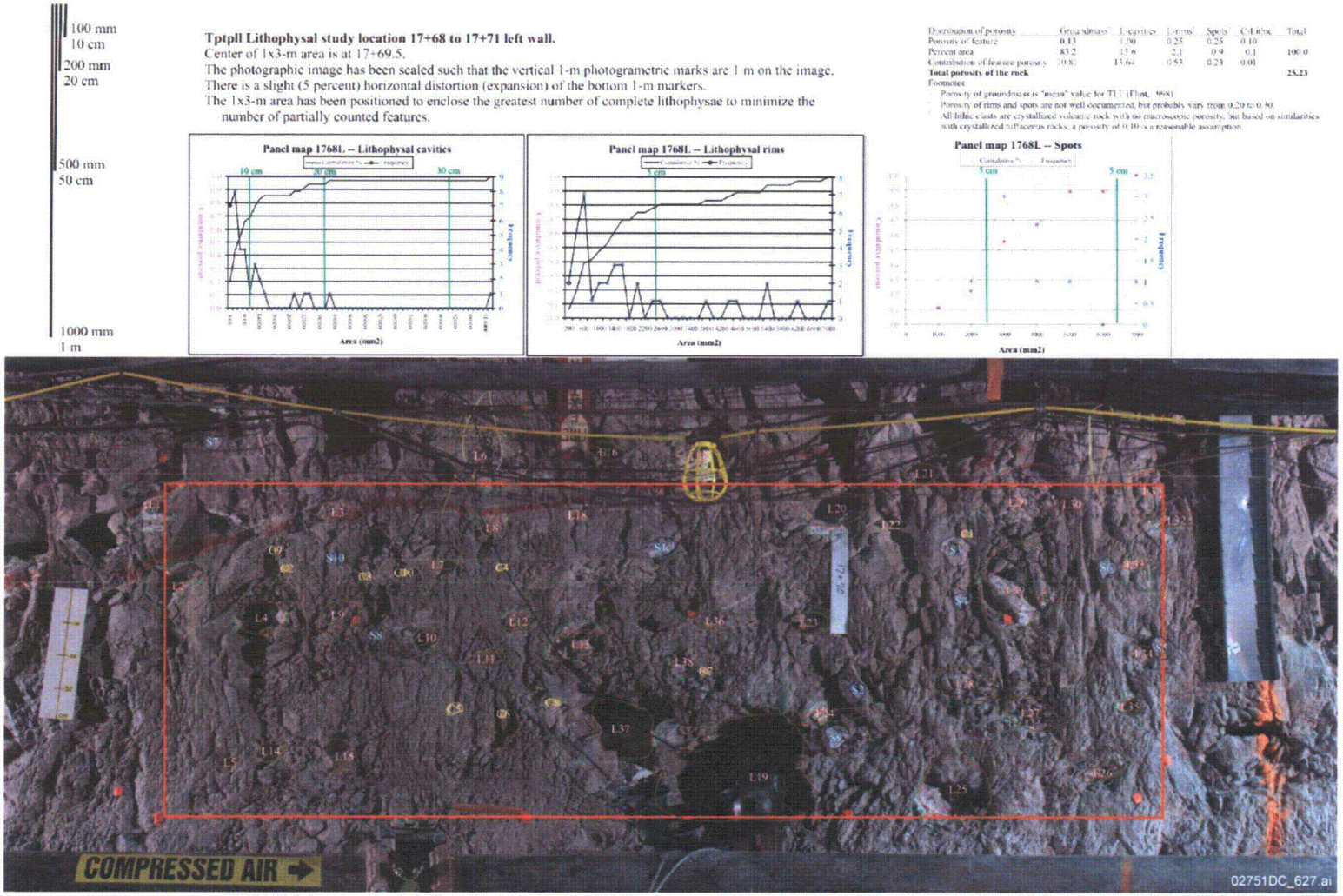

Source: BSC 2005, Figure A3-9.

Figure A-6. Positions and Sizes of Lithostratigraphic Features in Panel Map at 17+68L (left wall)

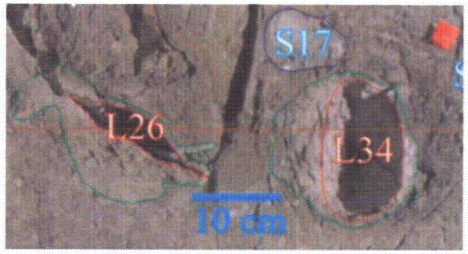

(a) "Simple" lithophysae (L34 & L26). (from Panel Map 1493R)

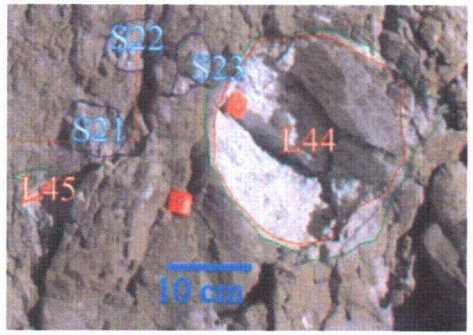

(b) "Simple" lithophysae (L45 & L44). L44 has small expansion cracks. (from Panel Map 1493R)

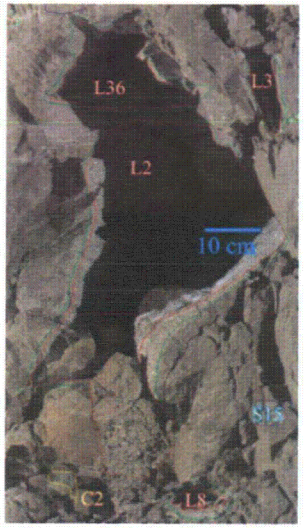

(c) Merged lithophysae (L2 & L36). (from Panel Map 1641L)
L2 itself is merged and has "backfilled" fracture at the base.

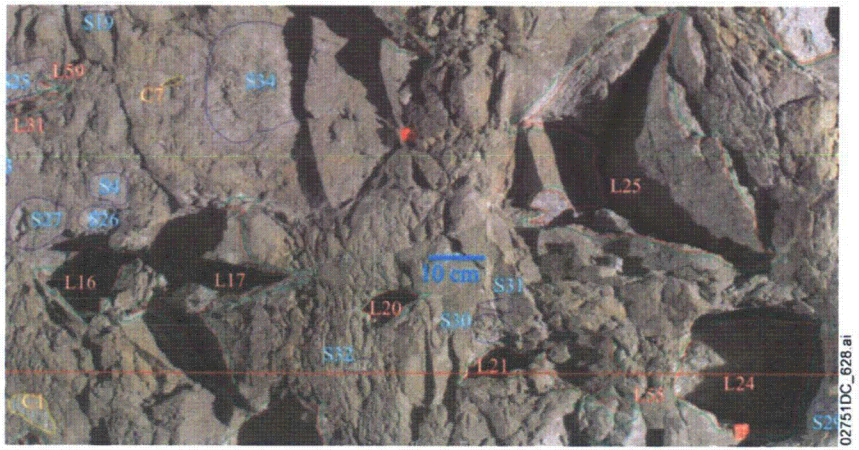

(d) "Expasion-crack" lithophysae (L15 & L25). Other lithophysae are "simple" shapes. (from Panel Map 1641L)

Source: BSC 2005, Figure A1-17.

Figure A-7. Shapes of Lithophysae

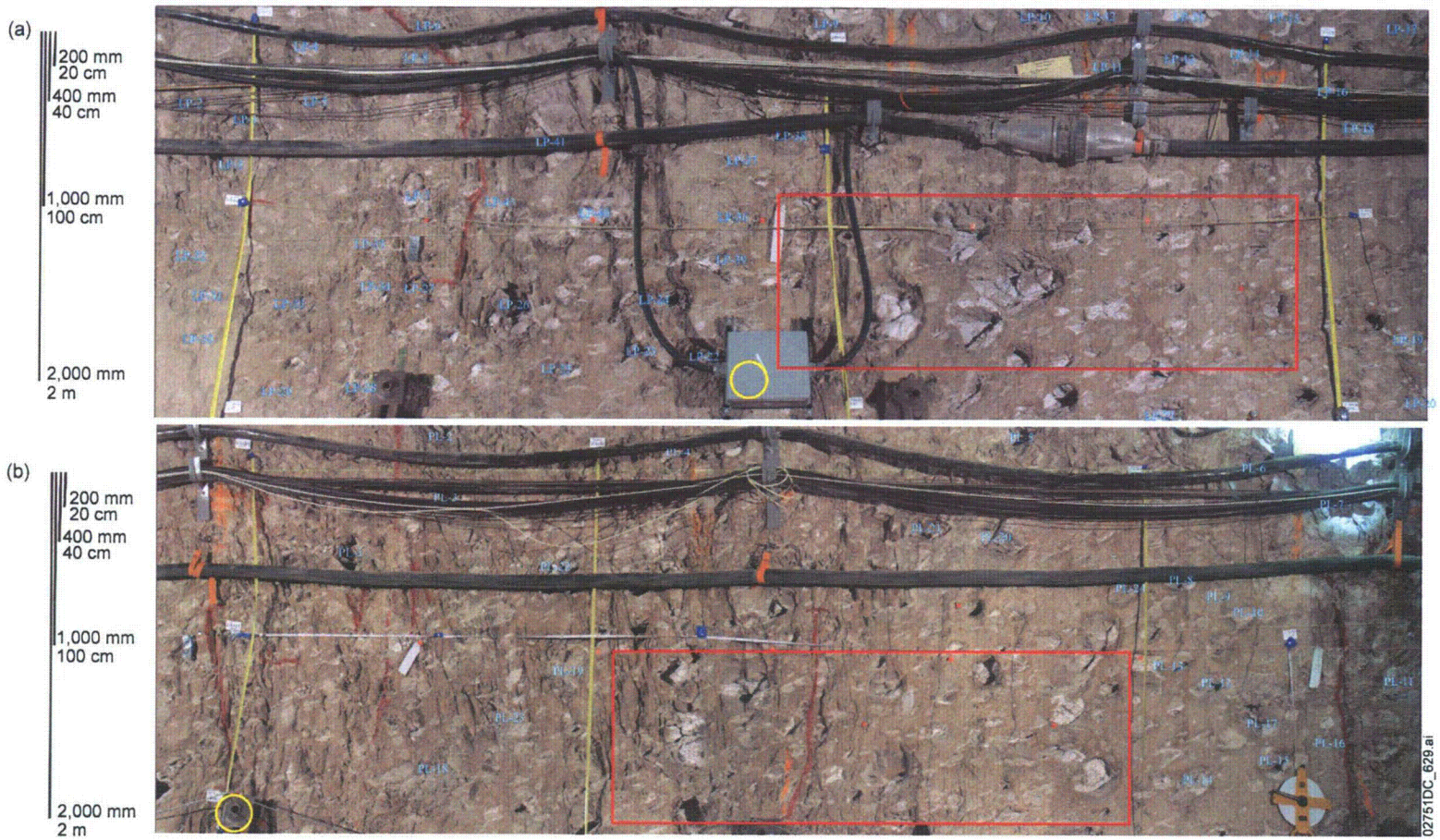

NOTES: Labeled lithophysae in Appendix D of BSC 2005; Figures A4-8 and A4-9 from BSC 2005.

Figure (a) is panel photograph at station 18+05 on left wall and small-scale fracture traverse location H7 with vertical traverses V19, V20, and V21 with lithophysae larger than 20 cm in diameter inventoried for shape and panel map 18+05L location indicated in red box (see Section A3 of BSC 2005).

Figure (b) is panel photograph at station 18+86 on left wall and small-scale fracture traverse location H8 and H9 with vertical traverses V22, V23, and V24 with lithophysae larger than 20 cm in diameter inventoried for shape and panel map 18+86L location indicated in red box (see Section A3 of BSC 2005)

Figure A-8. Panel Photograph at Station 18+05 and 18+86 on Left Wall with Lithophysae Larger Than 20 cm in Diameter

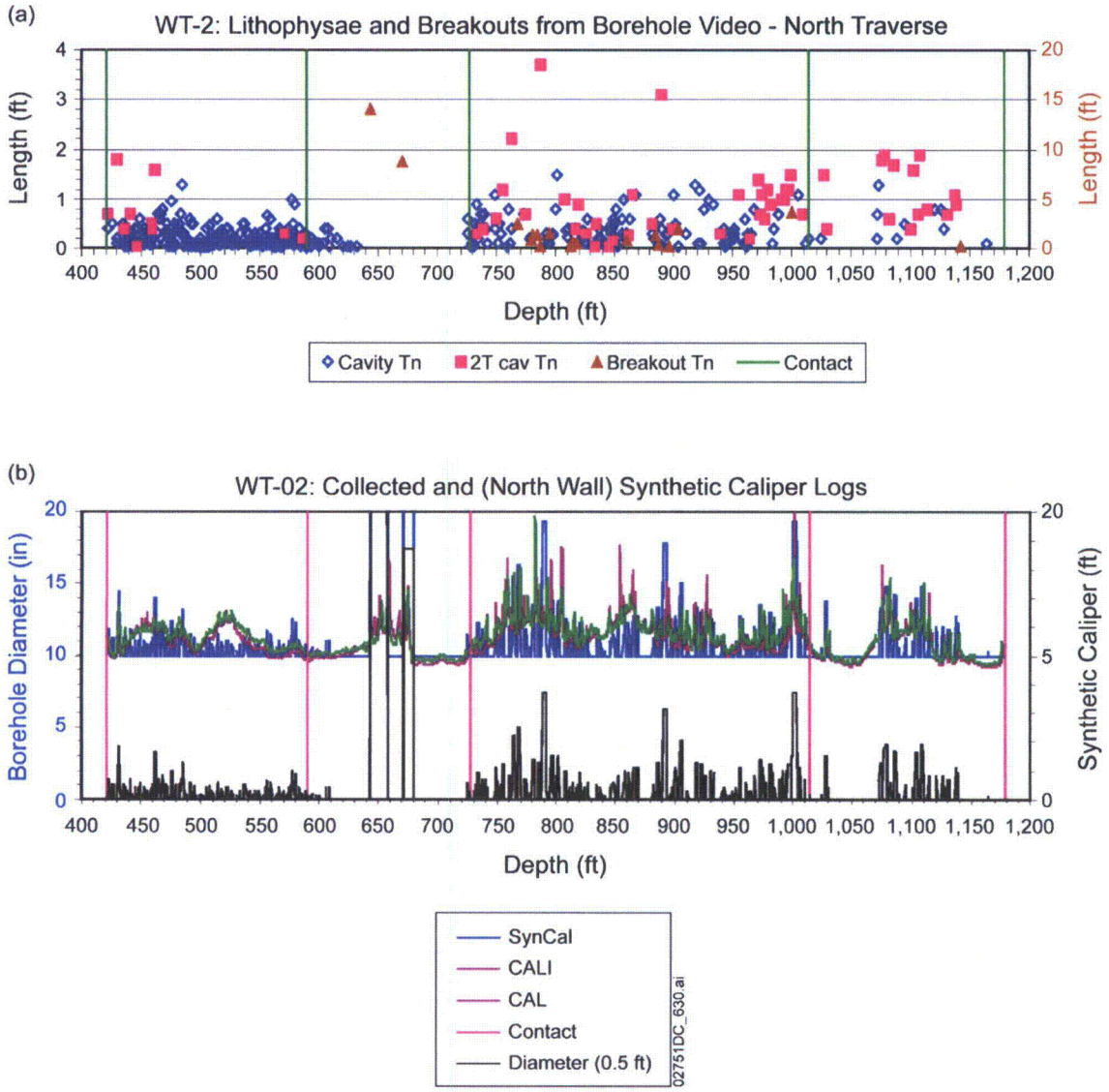

NOTES: Figure (a) is depth and length (both in feet) of lithophysal cavities (Cavity Tn), "big" lithophysae that are transected by at least 2 traverses (2 T cav Tn), borehole breakouts (Breakout Tn), and lithostratigraphic contacts (Contact) along the north traverse.

Figure (b) is of borehole diameters from synthetic caliper (SynCal) and geophysical caliper data (CALI and CAL) (all in inches) and lithostratigraphic contacts (Contact) along the north traverse. Synthetic caliper (Dia. 05 ft) is measured in feet for data at 0.5-ft increments (increments used to correlate to geophysical log data) and is plotted relative to 0 ft to indicate the difference between a straight wall and the relief of the wall surface caused by the lithophysae.

Figure A-9. Measured Lithophysal Cavities and Borehole Breakouts in Borehole USW WT-2 with Measured and Synthetic Caliper Data

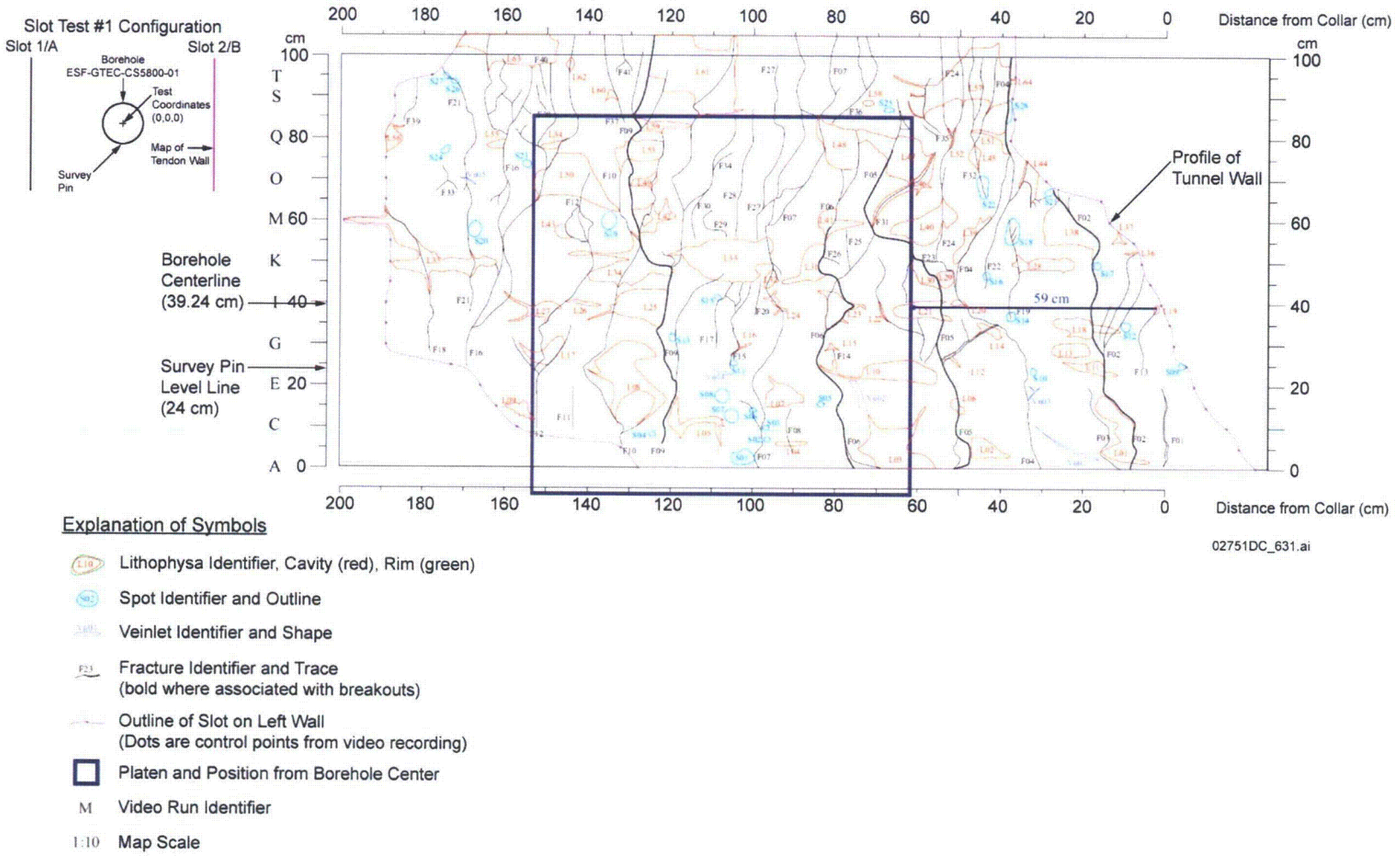

Explanation of Symbols

- Lithophysa Identifier, Cavity (red), Rim (green)
- Spot Identifier and Outline
- Veinlet Identifier and Shape
- Fracture Identifier and Trace (bold where associated with breakouts)
- Outline of Slot on Left Wall (Dots are control points from video recording)
- Platen and Position from Borehole Center
- M — Video Run Identifier
- 1:10 — Map Scale

Figure A-10. Geologic Map of Slot 2/B in Slot Test #1 in the Tptpll at ESF Station 57+77

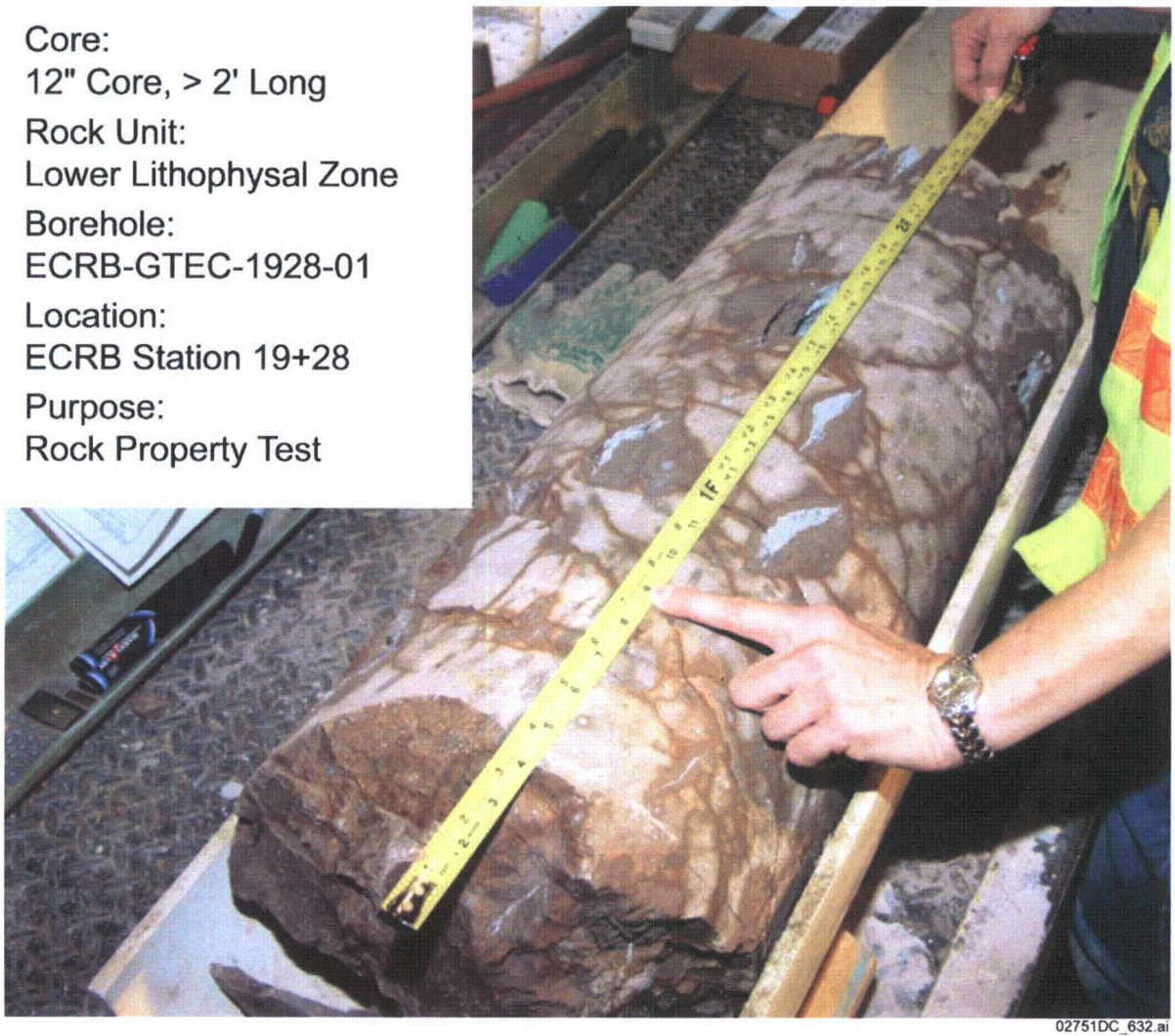

Source: BSC 2004, Figure 7-1.

NOTE: The core was drilled with water and the porous rims and fractures (many of which have rims) retain water and appear dark, whereas the matrix-groundmass, which has minimal porosity, dries in a relatively short amount of time. The foliation of the tuff, as defined by the elongation of lithophysal cavities and smaller crystallization features, dips down and to the left (away from the geologist). Fractures have a variety of orientations and trace lengths. The tape includes marks in feet and meters.

Figure A-11. Lithophysae and Fractures in Core of Tptpll from Borehole ECRB-GTEC-1928-01

A.3 SIGNIFICANT RESULTS FROM LITHOPHYSAL DATA

As summarized in this appendix, data on lithostratigraphic features such as lithophysal cavities, rims, spots, and lithic clasts have been collected from numerous studies that document these features in (1) several locations in the tunnels and surface-based boreholes, (2) different dimensions such as one-dimensional data (length only), two-dimensional data (areas), and locally three-dimensional data (volume), and (3) at a variety of scales from millimeters to hundreds of meters. There are several significant results from these studies:

- Lithophysae have a variety of shapes from smooth and spherical to very irregular.
- Lithophysal cavities typically range in size from about 1 cm to 1.8 m as observed in the ECRB Cross Drift. However, some of the detailed studies indicate lithophysae as small as several millimeters (that is, they have a 1- to 2-mm cavity, a rim, and vapor-phase mineral lining of the cavity), and other lithophysae are at least several decimeters in size (and this measurement is limited by the (1) geometry and size of the borehole or slot examined, or (2) minimum or maximum sizes used during data collection, and both of these limitations result in truncated data).
- The shapes of lithophysal cavities indicate that the larger lithophysae tend to be closer to circular in cross section whereas smaller lithophysae (those less than about 0.5 m in diameter) can also be nearly circular in cross section, but many are more elliptical in cross section (and some are very elongate).
- In the ECRB Cross Drift, data on the orientations of the long axes of lithophysal cavities indicate that the long axes are generally subhorizontal and, within ±20 degrees, similar to the orientation of the compaction foliation of the Topopah Spring Tuff.
- Distances between lithophysae can vary from centimeters to several meters, and some of this spacing depends of the size of lithophysae measured; for example, centimeter-sized lithophysae are typically centimeters to decimeters apart and decimeter-sized lithophysae are typically decimeters to several meters apart. However, there are many examples of centimeter- and decimeter-sized lithophysae being adjacent to each other.
- The ranges in abundance, size, and spatial data of lithophysae, which can also be represented as porosity, create a fabric of the rock that varies locally within 1- to 5-m^2 (or even 10-m^2) areas on the tunnel walls of the ECRB Cross Drift, and these local variations represent heterogeneities in the fabric of the rock. However, comparison of nearby measurements (within 10 to 30 m) indicates similar types of variations, and at these lengths along the tunnel, the fabric of the rock can be represented as homogeneous. Alternatively, on longer length scales along the tunnel (such as 50 to 100 m), the ranges in abundance, size, and spatial data typically differ because of the stratiform (informal subzone) relations within the Tptpll.
- The classification of lithophysal rocks into five categories, which were correlated to physical and mechanical properties (BSC 2004, Section E4.1.4.1; SAR Section 2.3.4.4.2.3.7) is representative of local conditions (5- to 15-m segments) along the ECRB Cross Drift and other local conditions documented along boreholes and in slot tests.

APPENDIX B
FRACTURE DATA

The fracture data are divided into primary input data and supporting data, which are described separately below. Because of the configuration of the ESF and ECRB Cross Drift, most of the data for the Tptpll are from the ECRB Cross Drift; however, some data are from the ESF and others are from surface-based boreholes. In relation to the shallowly dipping lithostratigraphic section at Yucca Mountain, including the Tptpll, the configuration of the ECRB Cross Drift results in a full lithostratigraphic section of the Tptpll being exposed in the ECRB Cross Drift (distributed along 882 m of tunnel).

Geologic studies document one- and two-dimensional distributions of fractures. The most used and cited data are summarized and developed in *Drift Degradation Analysis* (BSC 2004); other reports such as *Subsurface Geotechnical Parameters Report* (BSC 2007) and *Peak Ground Velocities for Seismic Events at Yucca Mountain, Nevada* (BSC 2005) also provide data on these lithostratigraphic features. In *Drift Degradation Analysis* (BSC 2004), most of the analysis of fracture data focused on the Detailed Line Survey (DLS) and Full Periphery Geologic Map (FPGM) data that represents only fractures with trace lengths greater than 1 m, and these data were used to develop the FracMan simulation.

B1 PRIMARY FRACTURE DATA FROM DETAILED LINE SURVEY (DLS) AND FULL PERIMETER GEOLOGIC MAP (FPGM) DATA

Primary fracture data from the DLS and FPGM data for the Tptpll represent only fractures with trace lengths greater than 1 m, and the orientation and trace length data are summarized in *Drift Degradation Analysis* (BSC 2004). Because of the configuration of the tunnels, most of the data from the Tptpll is from the ECRB Cross Drift. In the ECRB Cross Drift, there is an inverse relation of lithophysal percentage and fracture frequency where the fracture frequency is the amount of fractures in 10-m increments along the tunnel (Mongano et al. 1999, Figure 13). A synthesis of the DLS and FPGM data from the Tptpll was compiled in the FracMan simulation as described in Appendix B of *Drift Degradation Analysis* (BSC 2004). A slightly different synthesis of the fracture data is developed and summarized by Smart et al. (2006).

The DLS data consist of data measured with specific techniques along line traverses, and typically (1) the line is at or near spring line (the vertical part of the tunnel wall), and (2) all fractures within a 30-cm-wide swath above and below the traverse line are measured. There are two types of DLS data: the "total-tunnel" DLS data, and Small-Scale Fracture (SSF) data.

- The "total-tunnel" DLS data were collected along the length of the tunnel and are typically referred to simply as the DLS data. Throughout most of the ESF and ECRB Cross Drift, the DLS data were collected with a minimum trace length cutoff of 1 m; however, periodically the minimum cutoff was 30 cm. In the "total-tunnel" DLS data, lengths of individual measurements were rounded to the nearest 1 cm. In the ECRB Cross Drift, the trace lengths of fractures from the DLS data are typically less than 25 m and there are some variations along the tunnel that reflect the different lithostratigraphic

units (Figure B-1(a)). Trace lengths of 300 fractures in the DLS data vary from 1 to 45 m (only data greater than 1 m were measured) with a mean length of 3.88 m and a median length of 1.88 m (Figure B-1(b)).

- The SSF data were collected with the same techniques as used with the DLS data; however, there was no minimum trace length of a fracture (that is, there was no truncation of the shorter trace lengths), and SSF data were collected at specific locations. In the SSF data, lengths of individual measurements were rounded to the nearest 1 mm. At each SSF location there is a 6-m-long horizontal traverse (which is the same alignment as the total-tunnel DLS traverse), and there are three 2-m-long, vertical traverses: one vertical traverse located at each end of the horizontal traverse and one in the middle of the horizontal traverse (Figure B-2). This configuration results in a 6-m horizontal traverse and a total of 6 m in the vertical traverses, and was designed to capture steeply and shallowly dipping fractures. The SSF data were collected in two stages. The first set of SSF data (locations 1 to 6) includes three locations in the Tptpll, was submitted in 1999, and used in analyses for *Subsurface Geotechnical Parameters Report* (BSC 2007) and an independent report, *Summary and Analysis of Subsurface Fracture Data from the Topopah Spring Tuff Upper Lithophysal, Middle Nonlithophysal, Lower Lithophysal, and Lower Nonlithophysal Zones at Yucca Mountain, Nevada* (Smart et al. 2006). The second set of SSF data (locations 7 to 16) was submitted in 2004, included six locations in the Tptpll, and was used qualitatively to describe the fracture characteristics of the Tptpll. In total, SSF data were collected at 14 locations in the ECRB Cross Drift: two in the Tptpul, two in the Tptpmn, nine in the Tptpll, and one in the Tptpln.

The SSF data were not developed very extensively; however, they were included in *Subsurface Geotechnical Parameters Report* (BSC 2007) and *Drift Degradation Analysis* (BSC 2004), and they were analyzed statistically by Smart et al. (2006). An example of the spacing and varied orientation of SSF data at station 20+19 in the Tptpll, which was collected in the second set of SSF data, is depicted in Figure B-2.

- Three of the horizontal SSF traverses in the Tptpll (traverses H3, H4, and H5) were evaluated, but no formal calculations were produced. The evaluation led to the following conclusions in *Drift Degradation Analysis* (BSC 2004, pp. 15 to 16): (1) small-scale fracture traverses in the Tptpll confirmed the close spacing and short trace lengths of fractures in this zone, (2) the intensity and short trace lengths of fractures in this zone create a texture that limits the potential block size in this zone, and (3) lithophysae and occasional horizontal fractures tend to create blocks with dimensions on the order of about 10 cm or less on a side. *Surface Geotechnical Parameters Report* (BSC 2007, Section 6.4.3.4.1, p. 6-170) concluded that "The fractures, which exist throughout the Tptpll, have a primary vertical orientation, and have lateral spacing of a few centimeters."

- Further insight into the distribution of fractures in SSF data comes from the Tptpmn in which the SSF data were compiled, and included one of the key-block analyses (BSC 2004). This summary (BSC 2004, Table 6-37 and Figure 6-105) shows that 51% of fractures are 20 cm or less in trace length, 64% of fractures are 30 cm or less in trace

length, and 84% of fractures are 1 m or less in trace length. In an independent analysis of the same SSF data from the Tptpll, in which different and additional adjustments were made, the median trace length is 20 cm (Smart et al. 2006, Table 3-5). When orientation sets are identified in the SSF data, mean and median trace lengths vary from 33 to 106 cm and 15 to 31 cm, respectively, and the mean and median true spacings vary from 7 to 19 cm and 4 to 12 cm, respectively (Smart et al. 2006, Table 3-5).

- In an independent analysis of SSF data from the Tptpll, in which different and additional adjustments were made compared to those typically used by DOE, the median trace length is 16 cm (Smart et al. 2006, Table 3-7). When orientation sets are identified in the SSF data, mean and median trace lengths vary from 19 to 63 cm and 12 to 19 cm, respectively, and the mean and median true spacings vary from 10 to 108 cm and 3 to 12 cm, respectively (Smart et al. 2006, Table 3-7). Thus, even though the estimated trace lengths and spacings in the Tptpll based on the SSF were not computed with detailed statistical programs (BSC 2004, pp. 15 to 16), the estimate is a reasonable approximation.

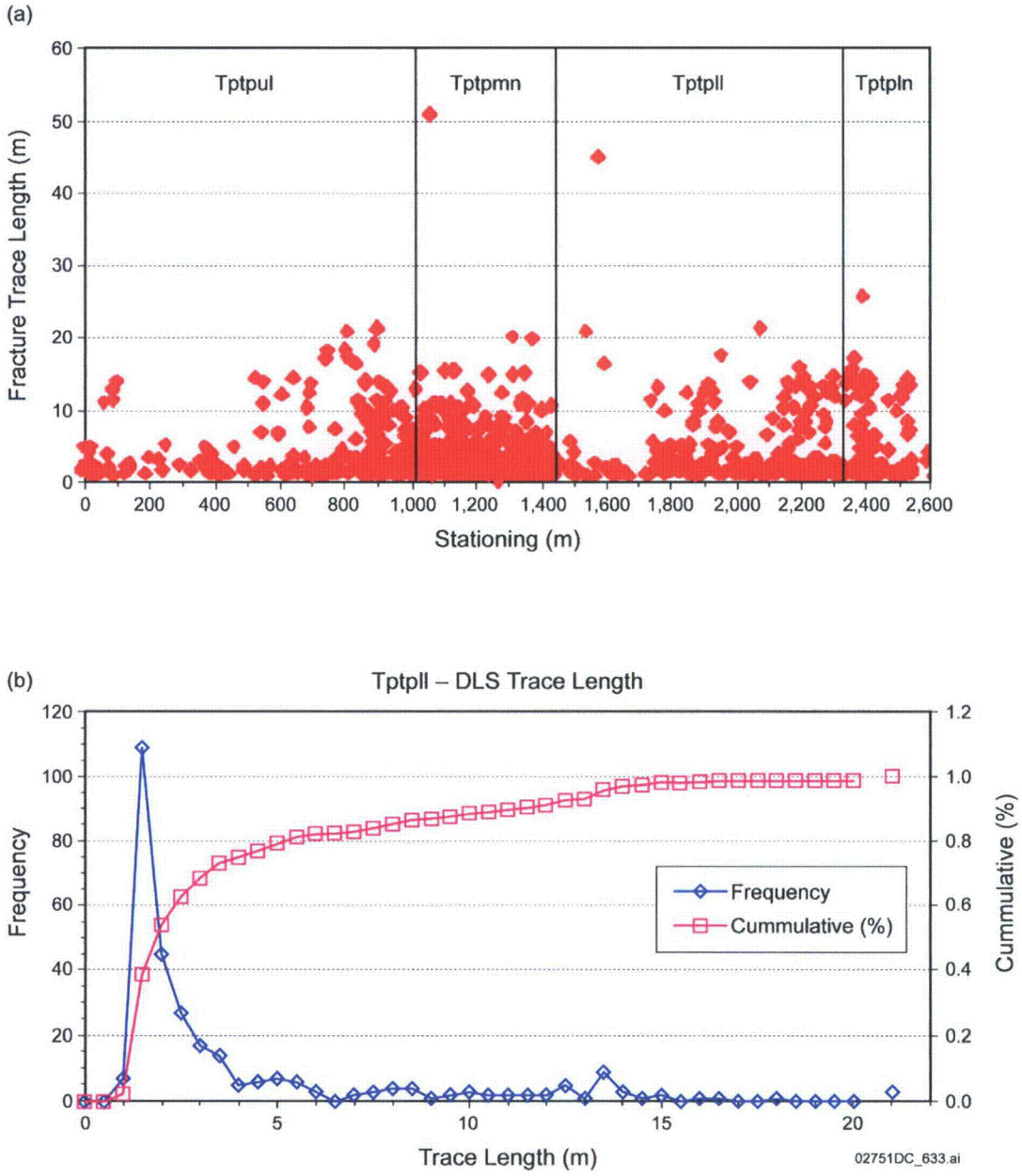

Source: See notes.

NOTES: DLS data of fractures with trace lengths greater than 1 m

Figure (a) is Figure 6-6 in BSC 2004.

Figure B-1. Fracture Trace Length from Detailed Line Surveys as a Function of Stationing along the ECRB Cross Drift and Trace Length Frequency in the Tptpll

Source: BSC 2005, Figure A1-19.

NOTES: Panel photograph at station location 20+19 on the left rib in the lower lithophysal zone with SSF data (trace lengths of fractures as yellow lines) and panel map data (lithophysal cavities, rims, spots, and lithic clasts) inside the 1 × 3-m red rectangle (lower right of photo).

Lithophysal cavities greater than 20 cm in diameter are labeled in cyan,

Red-painted lines (far left) are fractures greater than 1 m in length that were mapped as part of the DLS.

SSF data are from horizontal traverses H10 and H11 and vertical traverses V25, V26, and V27.

Figure B-2. Panel Photograph with SSF Data and Locations of Lithophysal Cavities Greater Than 20 cm in Diameter That Were Inventoried for Shape and Possible Collapse Features

B2 SUPPORTING FRACTURE DATA

Supporting fracture data are from: (1) details in the DLS and SSF data, (2) lithophysal panel maps, (3) fractures in rock slabs, (4) maps based on analysis of borehole video in the thermal conductivity tests and slot tests, (5) photographs of core and boreholes from the GETC-series of boreholes, and (6) Sample Management Facility geologic logs for the GETC-series boreholes.

B2.1 DLS and SSF data for the Tptpll in the ECRB Cross Drift

Supporting fracture data from DLS and SSF files for the Tptpll in the ECRB Cross Drift include a variety of data that typically were not summarized in other documents; however, these data include numerous attributes about the fractures, especially orientations, fracture lengths, terminations, and apertures.

- Orientation data – Orientation of fractures in the Tptpll from the SSF is similar to the total-tunnel DLS data; however, the SSF values are more diverse. Figure B-3 depicts the strike and dip values for individual SSF and total-tunnel DLS data in the Tptpll. The figure also includes mean strike and dip values for the SSF data with three sets at 134°/82°, 079°/82°, and 313°/04° and a fourth set of "random" fractures that were determined by Smart et al. (2006). For comparison, Figure B-3 also includes mean strike and dip values for the DLS data (fractures greater than 1-m trace length), with four sets at 329°/14°, 130°/80°, 175°/80°, and 278°/85° that were determined in *Drift Degradation Analysis* (BSC 2004).

- Trace length data –Trace lengths of 1,432 fractures in the SSF data vary from 0.016 to 21.4 m (there was no minimum trace length), with a mean length of 0.281 m and a median length of 0.140 m (Figure B-4). These data include all values from the horizontal and vertical traverses, and they were not separated into fracture sets (a practice done with many studies of fractures, including the evaluation by Smart et al. 2006).

- Terminations of fractures data – DLS and SSF files contain data on the numbers and types of terminations of the ends of fractures, and although there are many detailed categories, they can be simplified into fractures that end (1) in rock (that is, the fracture tip is visible with rock on three sides), (2) at a lithophysa, (3) at another fracture, or (4) that is obscured (or not visible), or (5) in a small number of other conditions (Table B-1).

- Aperture data – Aperture data (which is the distance between and perpendicular to the fracture walls or the mineral lining along fracture walls) are typically measured in 1-mm increments, and all fractures have measurements of the minimum and maximum apertures. Aperture along a fracture can be relatively complicated in detail and difficult to quantify; however, the minimum and maximum measurements provide a simple representation of the aperture. DLS data (fractures with trace length greater than 1 m) from the Tptpll indicate that approximately 44% of the fractures have apertures of 0 mm; therefore, approximately 56% of the fractures have apertures of 1 mm or greater (Figure 19 in Mongano et al. 1999). Aperture from the DLS and SSF data are

summarized in Table B-2. An aperture of greater than 0 mm is consistent with a lack of cohesion along the segment of the fracture.

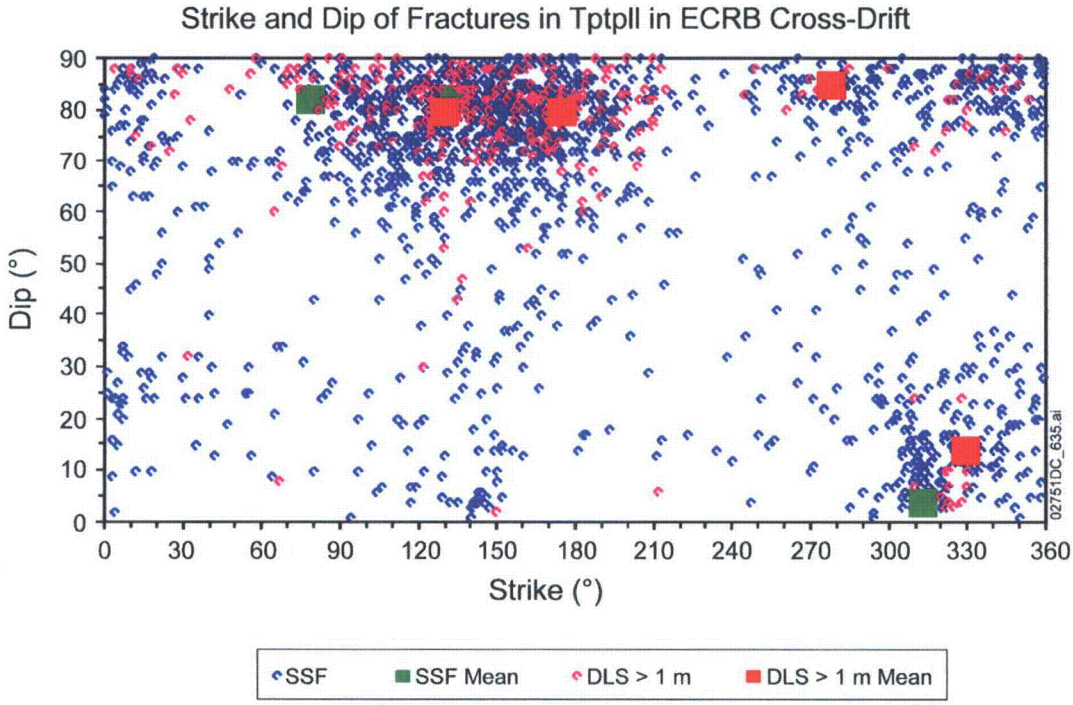

Figure B-3. Strike and Dip Data from SSF and Total-Tunnel DLS Data for the Tptpll in the ECRB Cross Drift

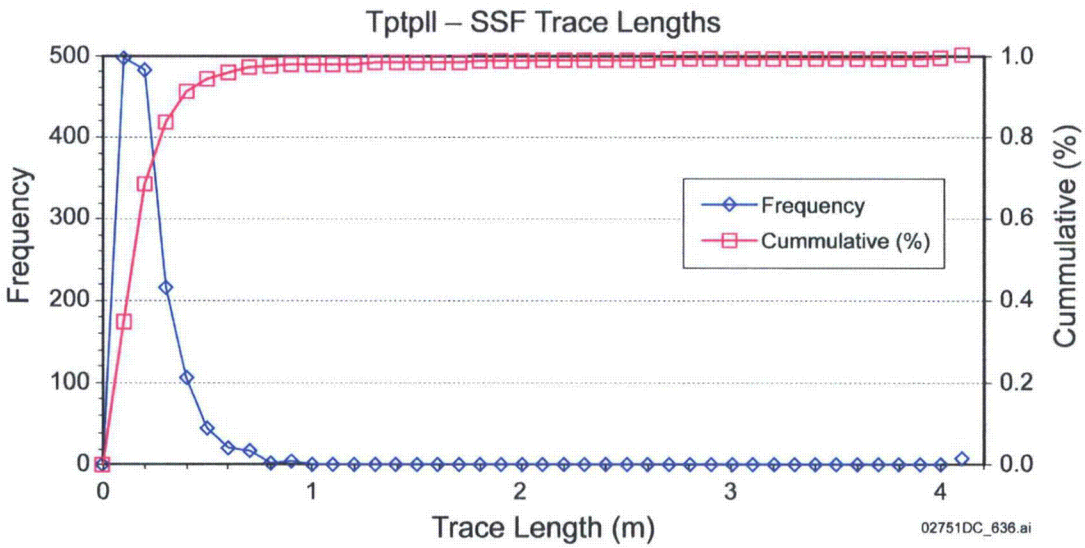

Figure B-4. Fracture Trace Length from Detailed Line Surveys as a Function of Stationing along the ECRB Cross Drift

Table B-1. Types of Terminations of Fractures in the Tptpll

	DLS (%)	SSF (%)
Number of ends visible		
2	58.5	87.4
1	31.2	10.1
0	10.0	1.7
other	0.3	0.8
Type of terminations		
another fracture	29.6	46.5
lithophysa	14.3	10.5
rock	30.4	35.5
obscured	25.4	1.5
other	0.3	6.0

Table B-2. Apertures of Fractures in the Tptpll

	DLS	SSF
Numbers of fractures	300	1444
Minimum aperture		
minimum	0 mm	0 mm
maximum	0 mm	5 mm
percent 0 mm	100.0 %	95.7 %
percent > 0 mm	0.0 %	2.6 %
percent "other"	0.0 %	1.4 %
Maximum aperture		
minimum	0 mm	0 mm
maximum	200 mm	30 mm
percent 0 mm	43.7 %	57.5 %
percent > 0 mm	56.3 %	40.8 %
percent "other"	0.0 %	1.6 %

B2.2 Fractures in Lithophysal Panel Maps and Panel Photographs

Although the panel maps compiled for the lithophysal studies did not include compilations of fractures, the photographs of the tunnel walls were used as base maps for the panels and provide photographic documentation of fractures. Lithophysal panel maps are available in DOE data, and photographs with panel map overlays are reproduced in *Drift Degradation Analysis* (BSC 2004, Figures O-3 to O-8) and *Peak Ground Velocities for Seismic Events at Yucca Mountain, Nevada* (BSC 2005, Figures A3-1 to A3-18). Additional photographs for SSF studies and panel photographs in the Tptpll are in *Peak Ground Velocities for Seismic Events at Yucca Mountain, Nevada* (BSC 2005, Figures A4-8 to A4-12).

Photographs for the panel maps and panel photographs that were used for examination of the relations of lithophysae and fractures for *Peak Ground Velocities for Seismic Events at Yucca Mountain, Nevada* (BSC 2005) represent only about 2% of the total exposed area of the tunnel walls. However, the locations of the photographs and related studies were identified as being representative of the rocks at various positions along the ECRB Cross Drift (BSC 2005).

The panel map at ECRB Cross Drift station 16+24 was used to map fractures based on photographic interpretation (Figure B-5). The fractures on this map were drawn for qualitative use. The 300 fractures in this panel map photograph have a variety of orientations (apparent dips in the face of the wall) and trace lengths. Some fractures intersect lithophysae or truncate into other fractures; however, many are in the matrix-groundmass and do not appear to be influenced by the occurrence of nearby lithophysae or other fractures.

There are several lithophysae-fracture relations, summarized below, for the 300 fractures depicted on the panel map at 16+24R (Figure B-5) and the 167 fractures depicted in the SSF data at 20+19L (Figure B-2; BSC 2005). Although detailed fractures have not been mapped, many of these relations are also in other panel maps and panel photographs (see Sections A3 and A4 of BSC 2005).

- Most fractures have trace lengths less than 30 cm, and only a few are greater than 50 cm.
- Most fractures are steeply dipping; however, those that appear to be more shallowly dipping might in fact be steeply dipping but with an apparent shallow dip in the plane of the tunnel cut.
- Many fractures have developed in the matrix-groundmass and appear to have formed irrespective of the occurrence of lithophysae nearby.
- Some fractures intersect or truncate into lithophysae, but few appear to transect lithophysae.
- Several fractures are "circum-lithophysal" fractures that formed around or parallel to the margins of lithophysae.

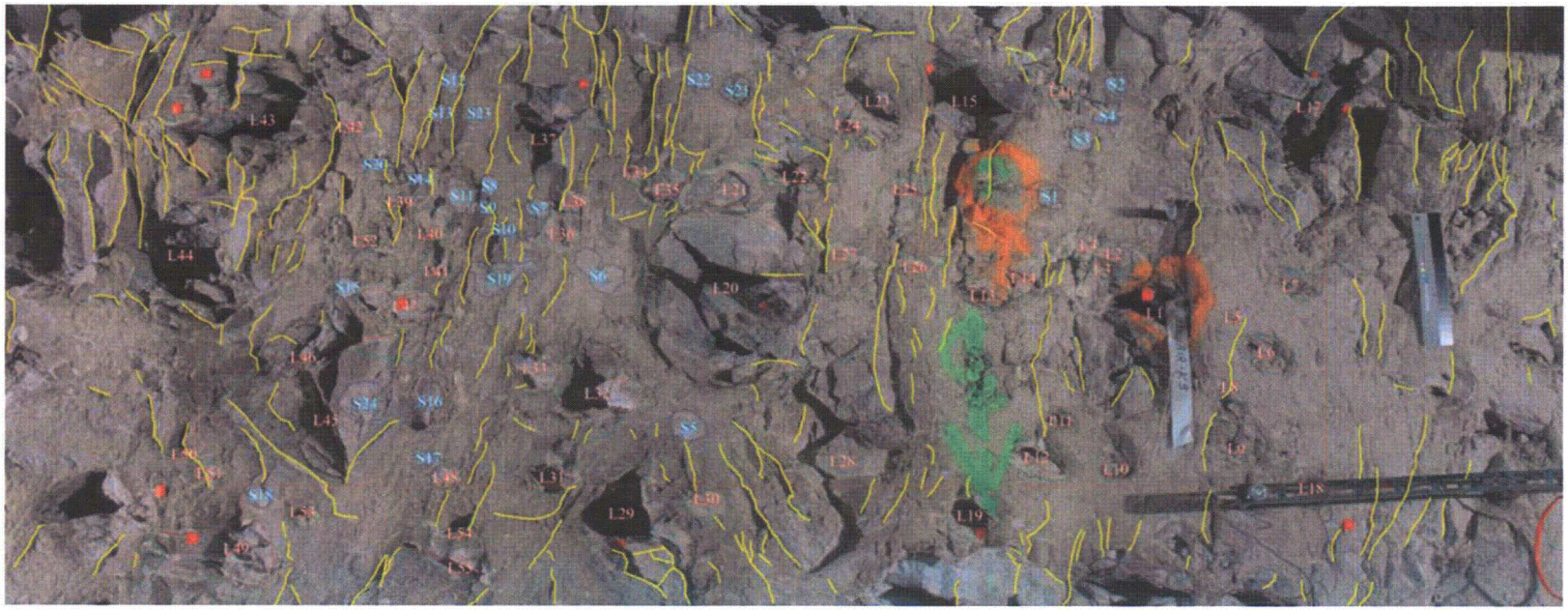

Source: BSC 2005, Figure A1-20a.

NOTE: Panel Map at 16+24 on the right wall with 300 photographically interpreted fractures (yellow lines).

Figure B-5. Photographic Interpretation of Fractures in the Lithophysal Rock at 16+24 in the ECRB Cross Drift

B2.3 Fractures in Rock Slabs

A rock slab is simply the surface (or face) of a rock exposed along a cut through a rock, and although the size of sample is not part of what designates a rock slab, in the context of the study of rocks from the Topopah Spring Tuff, the slabs are of core pieces from boreholes. Fractures in rock slabs of core include: (1) lithostratigraphic features, including vapor-phase mineral linings, rims, borders, or none of these features; and (2) fractures that have geometric relations such as terminations in rock or into other fractures or lithophysae, surface roughness, aperture and, rarely, separations along fractures. Data on fractures in slabs are summarized in *Peak Ground Velocities for Seismic Events at Yucca Mountain, Nevada* (BSC 2005). Samples for mapping of fractures on slabs of core were collected from two surface-based boreholes (including USW NRG-6 and USW UZ-14) and 32 tunnel-based boreholes (included Thermal Conductivity ["Therm-K,"] and Geotechnical [GTEC] boreholes) located in the ESF Main-Drift and the ECRB Cross Drift. The core from USW NRG-6 and USW UZ-14 is 61 mm in diameter, the Therm-K boreholes are 45 mm in diameter, and the GTEC boreholes are 289 mm in diameter. Because boreholes USW NRG-6 and USW UZ-14 are effectively vertical, the slabs of core were cut parallel to the core axis. Because the Therm-K and GTEC boreholes are effectively horizontal, the slabs of core were cut perpendicular to the core axis. Some of the slabs from the GTEC boreholes are only part of the full slab (that is, they are only one-quarter to one-half of the full diameter profile). Samples are from 10 lithostratigraphic zones and subzones in the Topopah Spring Tuff, and 45 samples are from the lower lithophysal zone (Tptpll). The areas of individual core slabs from the Tptpll varied from 9.5 to 157.2 cm^2.

Data on the fractures in rock slabs of core have been presented as colored maps where the different features (or groups of features) along fractures are depicted with different colors of lines (Table B-3, Figure B-6). Examples of fracture maps of core are from: (1) the upper lithophysal and middle nonlithophysal zones of the Topopah Spring Tuff in the borehole UZ-14, and (2) the lower lithophysal zone of the Topopah Spring Tuff in boreholes Therm-K-005 and Therm-K-007 (Figure B-6). Maps of slabs depict 10 fracture categories and geometric relations.

Seven typical relations of fractures in rock slabs, which are depicted in Figure B-6, are:

- Many fractures have a visible aperture; however, the amount was not measured. Some fractures have no visible aperture, and these include fractures that are filled with vapor-phase minerals (Figure B-7), "hairline fractures" that are filled with vapor-phase minerals, fractures that are annealed, and streaks (Table B-3). A streak typically has the rim and border crystallization characteristics similar to a veinlet; however, it does not have a fracture with an aperture that is filled (or partially filled) with vapor phase minerals. A streak is an incipient fracture; that is, it either had a narrow fracture along which the vapor phase flowed and reacted with a glassy host rock to form the rim and border crystallization, but the original fracture was obscured by subsequent crystallization, or the vapor phase simply migrated along a path that did not have an original discrete fracture.

- Many fractures are of a single category; however, some fractures have different crystallization characteristics along their trace. Typically, variations occur along fractures in the development of the rims or vapor-phase mineral coatings.

- Some fractures have trace lengths that transect the core; however, many fractures have trace lengths and terminations completely within the core. For fractures that are longer than the core, the "true" trace length is not known and the recorded length is a truncated value.

- Some fractures intersect or terminate at other fractures or lithophysae, whereas many fractures terminate in the rock. Fracture intersections and terminations occur at angles ranging from acute, to 90°, to obtuse. Some fractures have several splays that either bifurcate or reconnect to form an anastomosing pattern, and not every "branch" along the fracture was counted individually.

- Although in the two-dimensional map view of the slabs of core, (1) some fractures transect the length of core, (2) there can be a fracture network, or (3) individual fractures are not connected to other features, the three-dimensional configuration of fractures must be such that the rock maintains integrity. After the slabs of core were cut, rarely did the slab continue to break or degrade.

- Although the maps are at a scale where features less than 1 mm can be identified, fractures rarely have evidence of lateral separation across them. Fractures do not have evidence of mechanical degradation such as brecciation or rounding of corners formed at the intersection of fractures.

- One of the purposes of identifying fractures in slabs of core was to use lithostratigraphic features to constrain the general timing of when the fracture and associated features formed, and the two general periods of time were: (1) during the cooling of the deposit and (2) after the deposit had cooled (which was categorized as "indeterminate"). At the scale of the slabs of core, features that are associated with processes that were active during the cooling of the deposit (especially in the welded and crystallized units such as the Tptpll) include vapor-phase minerals, rims, spots, borders, and color of adjacent matrix-groundmass. If none of these features was associated with a fracture, it was categorized as" indeterminate."

Table B-3. Categories of Fractures Based on Development of Lithostratigraphic Features

Symbol	Color	Description
VPLm-w, R	Cyan	Vapor-phase lining (VPL) is moderately to well developed, Rims (R) are well developed.
VPLp, Rp	Green	VPL and R are poorly developed.
VPLhair	Deep Blue	VPL in (fills) hairline fractures
VPLn, Rp	Chartreuse	No VPL, Rims or borders are poorly developed.
VPLn, Rn, An	Brown	No VPL or R, but fracture is annealed.
Veinlet	Magenta	Veinlet (pathways of vapor-phase transport) that has VPL
Streak	Magenta	Fracture (many are incipient) with rim material, but no VPL
P or B border	Gold	Purple or brown borders on fractures, but with no VPL
VPLn, Rn	Black	No VPL or R and no other mineral lining, so the timing of fracture formation is indeterminate.
B min	Red	Black mineral deposits along fracture surface (presumably manganese or iron oxides), so the timing of fracture formation is indeterminate.

(a)

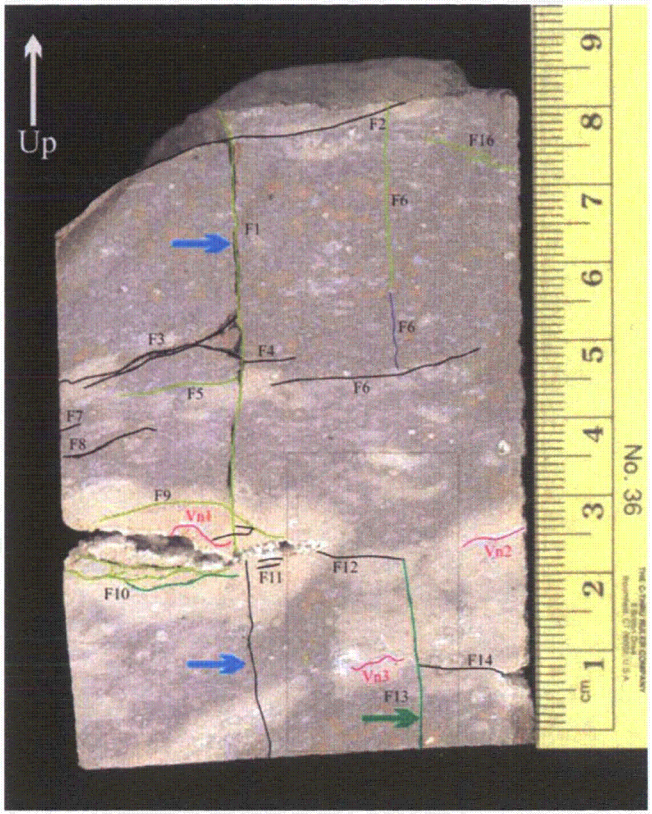

Fractures traced as "hairline" fractures to the outer wall of core are indicated with cyan and green colored arrows. Fracture (cyan line) also intersects the same lithophysal cavity on core wall with a similar "jog". The two fractures in the upper left have thin coatings of colorless euhedral (vapor-phase or zeolite) minerals. Fracture (green arrow) terminates in rock on outer wall and has a small amount of white (vapor-phase?) mineral filling at terminus.

UZ-14 714.1 ft, Tptpul (sample number 0029744)

(b)

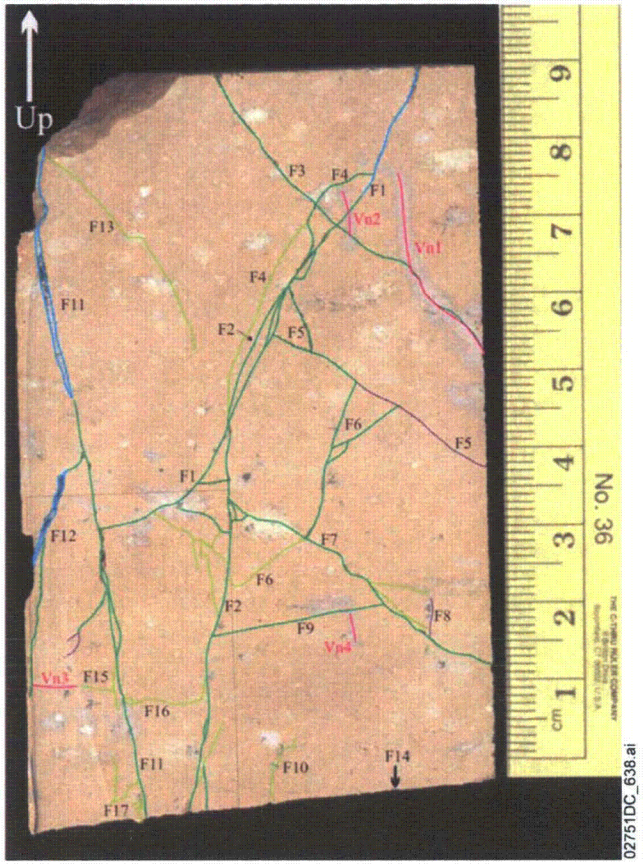

UZ-14 732.2 ft, Tptpmn3 (sample number 0029749)

Source: BSC 2005, Figure A1-5.

NOTES: In Figure (a), slab is from the upper lithophysal zone at a depth of 714.1 ft in USW UZ-14.

In Figure (b), slab is from the middle nonlithophysal zone (specifically the upper nonlithophysal subzone) at a depth of 732.2 ft in USW UZ-14.

Color codes for fractures are listed in Table B-3.

Figure B-6. Fracture Maps of Core from Boreholes USW UZ-14 and Therm-K-005 and Therm-K-007

Therm-K-007 0.4 ft, Tptpll (sample number 01013319)

Therm-K-005 40.1 ft, Tptpll (sample number 01013269)

Source: BSC 2005, Figure A1-5.

NOTES: In Figure (c), slab is from the lower lithophysal zone at a depth of 0.4 ft in Therm-K-007.

In Figure (d), slab is from the lower lithophysal zone at a depth of 40.1 ft in Therm-K-005.

Color codes for fractures are listed in Table B-3.

Figure B-6. Fracture Maps of Core from Boreholes USW UZ-14 and Therm-K-005 and Therm-K-007 (continued)

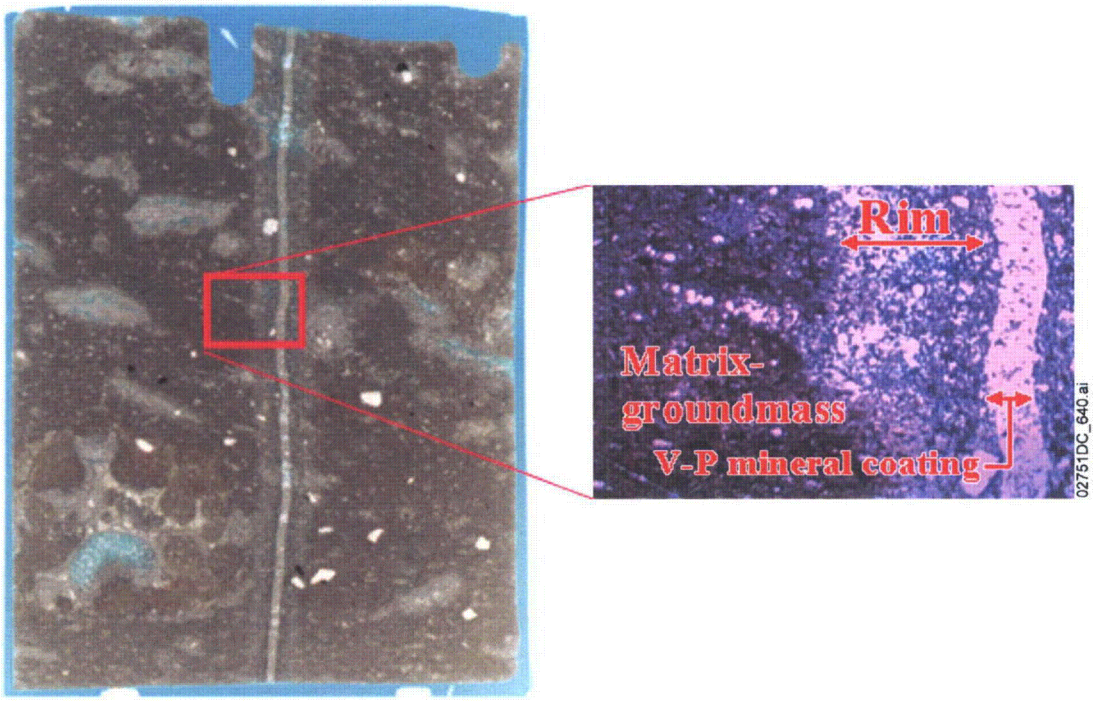

NOTES: The thin section is approximately 21 × 27 mm, and is oriented vertically with the top of the section toward the top of the formation. The thin section is impregnated with blue epoxy, and this slightly affects the colors of the rock. The matrix-groundmass is brown (7.5YR5/2) crystallized ignimbrite. The vertical fracture is slightly smooth, has a well-developed rim (light gray to pink, 5-7.5YR7/1-3), with a colorless to white vapor-phase mineral coating filling the fracture.

Detailed relations of matrix-groundmass, rim, and vapor-phase mineral filling are enlarged red rectangle.

Sample (SMF) identification number is 0028274.

Figure B-7. Fracture Filled with Vapor-Phase Minerals in a Thin Section of Core from Tptpmn in Borehole NRG-6 at a Depth of 730.2 ft

Data on the fractures in rock slabs of core have been presented as graphs depicting various properties of the fractures. In the graphs, lithostratigraphic units are depicted using short symbols or numerical values, and these are summarized in Table B-4. One set of graphs depicts the trace lengths of fractures that are classified as those with trace lengths equal to or greater than 1 cm and those less than 1 cm (Figure B-8). The number of fractures per unit area (cm^2) of slab varies by lithostratigraphic zone and subzone with the: (1) larger values in the deepest part of the section and (2) the lower lithophysal zone having the larger individual values (Figure B-8(a)). These trends are similar where the fractures are divided into fractures longer than 1 cm and especially for those that are shorter than 1 cm (Figure B-8(b) and (c)). Similar relations of the total area and total fractures per total area compared to the lithostratigraphic zone or subzone also indicate that the lower parts of the section, especially the lower lithophysal zone, have more fractures per unit area than the upper parts of the section (Figure B-9). Because there are only a few samples from lithostratigraphic units other than the upper and lower lithophysal zones (for example, Tptrv to Tptrl, Tptpmn, and Tptpln in Table B-4), some bias to smaller values of the "total fracture per total area" data for the minimally represented units is possible. Alternatively, there are numerous samples from the Tptpul and Tptpll, both in number and total area (Table B-4

and Figure B-9); therefore, comparisons (especially of these two units) do not contain any bias. These fractures-per-area relations indicate that the various lithostratigraphic units responded differently in the formation of fractures and support the stratiform characterization of fractures.

Table B-4. Number of Core Samples in Lithostratigraphic Zones and Subzones of the Topopah Spring Tuff

Lithostratigraphic Unit	Symbol[a]	Short Symbol	Unit Number[b]	Number of Samples
Crystal-rich member	Tptr	—	—	—
Vitric zone	Tptrv	—	—	—
Densely welded subzone	Tptrv1	rv1	8.2	2
Nonlithophysal zone	Tptrn	rn	7.0	6
Lithophysal zone	Tptrl	—	—	—
Crystal-rich subzone	Tptrl2	rl2	6.4	1
Transition subzone	Tptrl1	rl1	6.2	1
Crystal-poor member	Tptp	—	—	—
Upper lithophysal zone (Therm-K)	Tptpul*TK	pul*TK	5.2	8
Upper lithophysal zone	Tptpul	pul	5.0	32
Middle nonlithophysal zone	Tptpmn	—	—	—
Transition subzone	Tptpmn4	pmn4	4.4	4
Upper nonlithophysal subzone	Tptpmn3	pmn3	4.3	1
Lower lithophysal zone (Therm-K)	Tptpll*TK	pll*TK	3.2	36
Lower lithophysal zone	Tptpll	pll	3.0	19
Lower nonlithophysal zone	Tptpln	pln	2.0	7
Vitric zone	Tptpv	—	—	—
Densely welded subzone	Tptpv3	pv3	1.6	3

[a] Lithostratigraphic names and symbols are from Buesch et al. 1996, Table 2, and Buesch and Spengler 1998, p. 16.

[b] "Unit number" is arbitrarily assigned to zones and subzones with the smallest number for the deepest units. "Unit number" is only used for plotting or sorting of data on the basis of lithostratigraphic zone or subzone. The ThermK samples have a unique number because they are from small-diameter core samples.

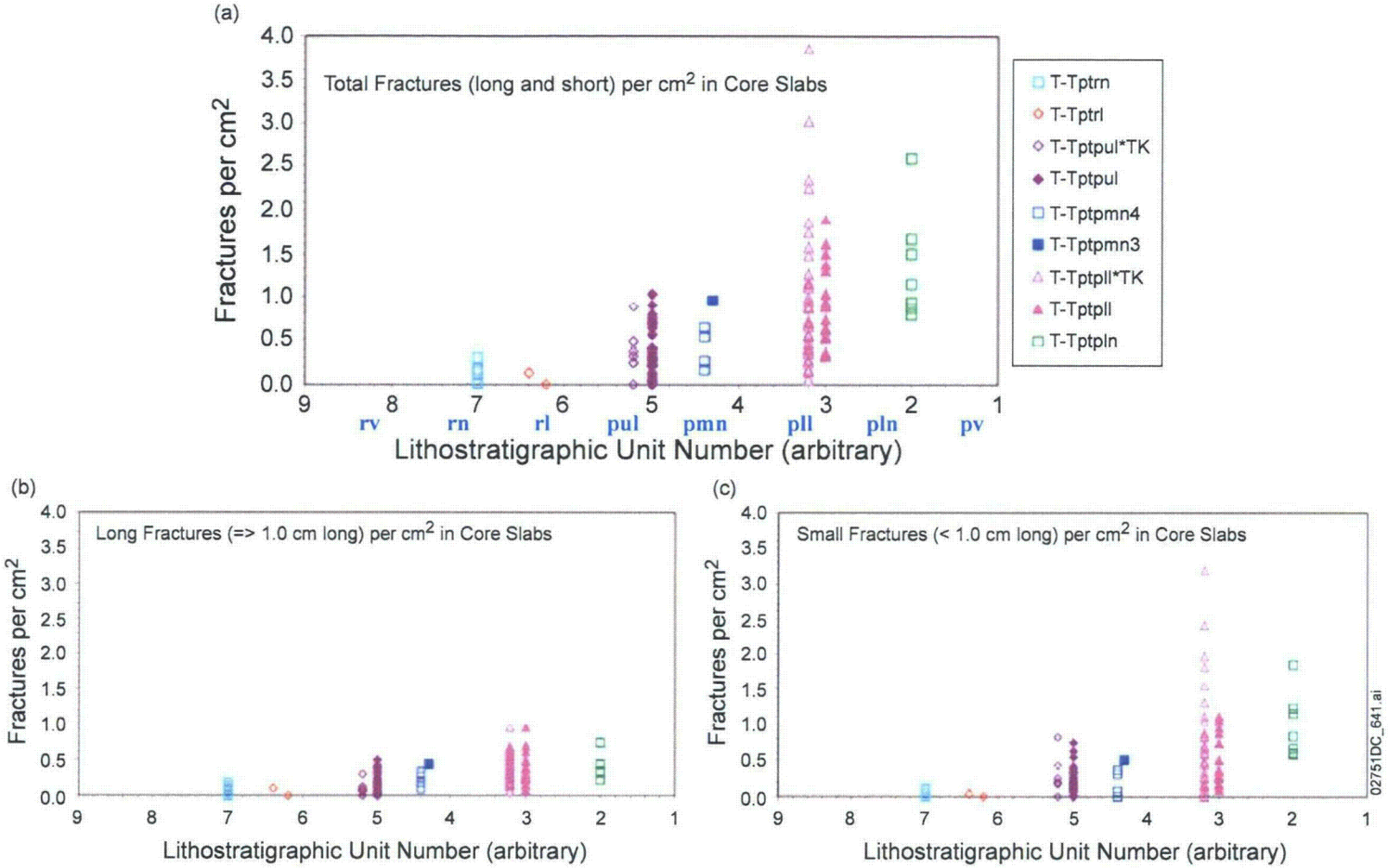

Source: BSC 2005, Figure A1-8.

NOTES: Figure (a) shows total number of fractures per cm^2 of slab by lithostratigraphic units. Symbols for lithostratigraphic units are in Table A1-2.
Figure (b) shows number of fractures greater than 1 cm long per cm^2 of slab by lithostratigraphic units.
Figure (c) shows number of fractures less than 1 cm long per cm^2 of slab by lithostratigraphic units.

Figure B-8. Variation in the Numbers of Fractures per Area (cm^2) of Slab by Lithostratigraphic Zone and Subzone

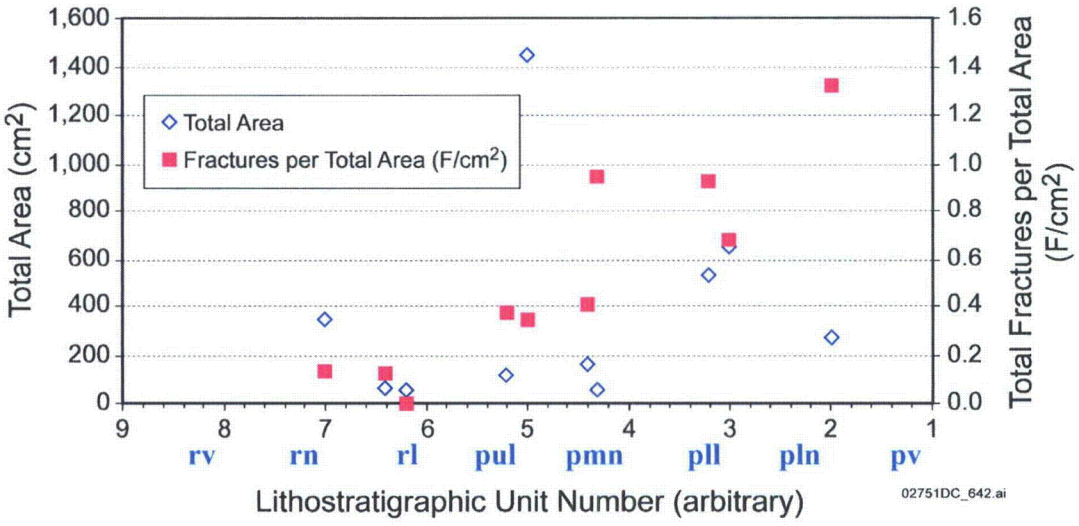

Source: BSC 2005, Figure A1-9.

NOTES: Total number of fractures per cm^2 of slab by lithostratigraphic units. Symbols for lithostratigraphic units are in Table A1-2.

Number of fractures greater than 1 cm long per cm^2 of slab by lithostratigraphic units.

Number of fractures less than 1 cm long per cm^2 of slab by lithostratigraphic units.

Figure B-9. Total Area of Samples and Total Number of Fractures per Total Area (cm^2) of Slab by Lithostratigraphic Zone and Subzone in Slabs of Core from the Densely Welded and Crystallized Topopah Spring Tuff

Fractures, with similar features and geometric relations as have been documented in slabs of core, have been identified in thin sections; however, photographs (or scanned images) of the thin sections have rarely been included in data packages or reports. Typically, thin sections are approximately 21 × 27 mm and provide very detailed views of the features in rocks. Two examples of fractures in thin sections of core samples from the Tptpll in borehole NRG-6 are shown in Figure B-10. During the preparation of these thin sections, they were impregnated with blue epoxy to enhance identification of pore space in the rock. Among many different lithostratigraphic features in the thin sections, numerous fractures are identified by the occurrence of rims, borders, vapor-phase mineral linings, or simply blue epoxy that filled small apertures. Typically, fractures have steep apparent dips, but some have more shallowly dipping apparent dips. In these thin sections, a few fractures are isolated (that is, they terminate in the surrounding matrix-groundmass); however, many of the fractures terminate into (or cross) other fractures, lithophysae, spots, or lithic clasts. Apertures of fractures were not systematically measured; however, apertures of 10 to 30 microns have been estimated in a number of thin sections. As with slabs of core, some fractures in the core resulted in the "plucking" of pieces of the chip during initial preparation; however, during the cutting of thin sections, rarely was there additional plucking.

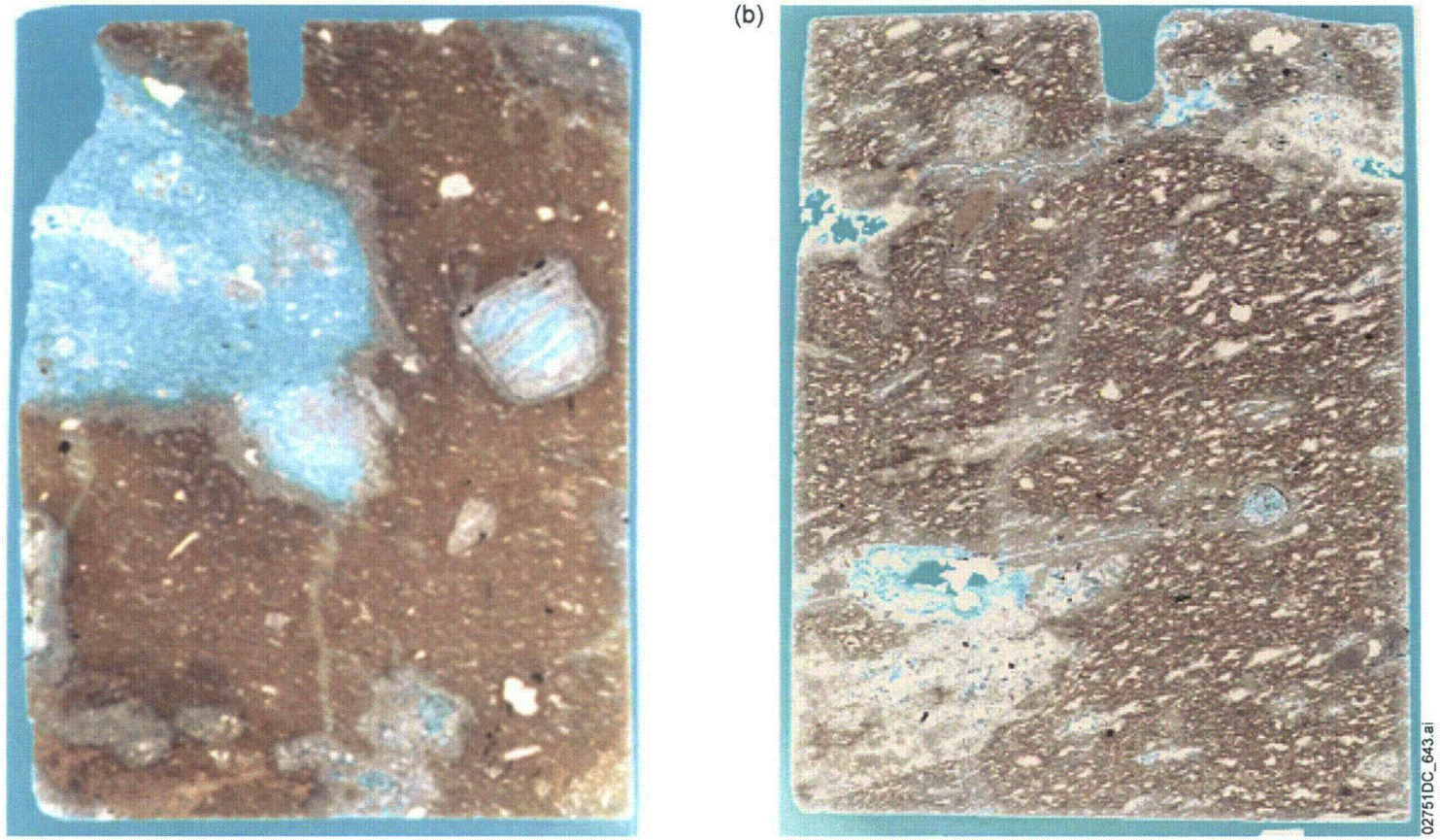

NOTES: Thin sections are approximately 21 x 27 mm, and are oriented vertically with the top of the section toward the top of the formation. The thin sections are impregnated with blue epoxy, and this slightly affects the colors of the rock. The matrix-groundmass is brown to pale brown (7.5YR5/2 to 10YR6/3) crystallized ignimbrite. Fractures are slightly smooth to slightly rough with moderate- to well-developed rims (light gray to pink, 5-7.5YR7/1-3), and a few have colorless to white vapor-phase mineral coating filling the fracture. Some pumice, lithic, and vitroclastic-shard clasts were vapor-phase corroded, and some have been (partially) filled with vapor-phase mineralization.

Sample (SMF) identification numbers are 0028281 for thin section (a) and 0028286 for thin section (b).

Figure B-10. Fractures in Thin Sections of Core from Tptpll in NRG-6 at Depths of 853.5 ft and 955.9 ft

Summary of relations for fractures in slabs of core and in thin section:

- Samples of core are from a variety of locations, some from surface-based boreholes and others from various depths in boreholes drilled in the ESF and ECRB Cross Drift; therefore, they represent various spatial and lithostratigraphic conditions of the lithostratigraphic units.

- Fractures occur in many rocks (especially those from the Tptpll) and at many different scales, even down to measurements at scales of centimeters and millimeters.

- Fractures have identifiable, although small, apertures at the scale of core and thin sections, some as small as 10 microns.

- Fractures can have a variety of trace lengths; however, the slabs of core and thin sections document an abundance of small trace lengths, especially in the Tptpll.

- The terminations of many fractures can be identified at one or both ends, and although many terminate at (or intersect) other fractures, lithophysae, spots, and even lithic clasts, some fractures terminate in the surrounding matrix-groundmass.

- Many fractures are steeply dipping (at least the apparent dip in the plane of the slab or thin section is steeply dipping); however, fractures of all orientations occur in individual samples.

- Slabs of core and thin sections indicate two-dimensional fracture networks that are variably developed in specific samples that consist of: (1) fractures connected to other fractures or lithostratigraphic features, and (2) rock "bridges" between fractures.

- Regardless of two-dimensional configurations, the three-dimensional samples of core remained intact during the cutting of core for slabs or thin sections. These conditions support the interpretations that although there are various amounts of small-scale features that might be activated during applied stresses on the rock and influence the mechanical or thermal properties of the rock, most of these samples represent good quality examples of the rock mass from which they were sampled.

- Most fractures in the slabs of core study, and in thin section, are associated with lithostratigraphic features such as vapor-phase minerals, rims, borders, spots, and color of adjacent matrix-groundmass that indicate the fracture and associated features formed during the period of time when the deposit was cooling. The importance of these observations is that most of the fractures formed during a relatively short period of time after the deposit was formed, and that they are throughout the rock mass.

B2.4 Fractures in Thermal-K and Slot Tests

Although the main goal of the analysis of video recordings in thermal conductivity tests and slot tests was to document lithophysae and related features (as described in Section 1.1.2.4), many of

the data files and maps also documented fractures. Because the analysis was based only on video recordings, many types of data related to fractures were not collected; however, some geometric relations can be inferred.

- In some boreholes, accumulations of dust preclude detailed analysis; however, in many of the video recordings there is sufficient clarity and quality to determine more detail on approximations of orientations of fractures; however, this was not the emphasis of the study and it was not done.

- Slot tests have photographs of the tunnel walls, and fractures can be identified on these photographs.

- Interactions of lithophysae, spots, and fractures are depicted on maps, for example, the map for Slot 2/B in slot test #1 in the Tptpll at ESF station 57+77 (Figure A-10). Some "plucking" of the walls during drilling might have enhanced the apparent apertures of some fractures and shapes of some lithophysal cavities, but where possible, the boundaries of lithophysal cavities and some fractures were identified by the occurrence of rims or vapor-phase mineral coatings.

- Most of the observations of fractures are restricted to individual boreholes or slots; however, because of the position and orientation of some fractures it was possible to infer the occurrence of fractures in more than one borehole or slot.

B2.5 Photographs of Core, Boreholes, and Other Test Locations

Photographs taken of core, boreholes, and other test locations provide local examples of lithostratigraphic features including lithophysae and fractures. Some photographs were taken as part of the documentation during field activities, including the recovery of core from boreholes, whereas other photographs were taken to demonstrate specific features or relations.

- In the piece of core from borehole ECRB-GTEC-1928-01 in the Tptpll from the ECRB Cross Drift (Figure A-11), fractures with various orientation and trace lengths are identified because of water retained in the apertures or in rims along the fracture margins.

- Examples of photographs taken to demonstrate specific features include those taken in GTEC-series boreholes that include fracturing in rocks of the lower lithophysal zone and no fracturing in rocks of the upper lithophysal zone (Figure B-11). Both boreholes are about 12 inches in diameter. Many of the fractures in the borehole in the Tptpll are approximately perpendicular (90°) to the borehole axis, which makes them nearly parallel to the wall of the tunnel. However, some fractures are at angles to the borehole axis. Some of the apparent apertures could have been enhanced during the drilling by plucking of material from edges of the fractures or breaking between two closely spaced fractures.

- Small-scale infiltration tests (referred to as "bench tests") were conducted at six locations in the ECRB Cross Drift, three of which were in the Tptpll. The test layouts consisted of a horizontal bench cut into the wall of the tunnel, with one or two 12-inch-diameter metal

cylinders that were used to pond the water for the infiltration measurements (Figure B-12(a)). Maps of fractures were made of the test areas (Figure B-12(b)).

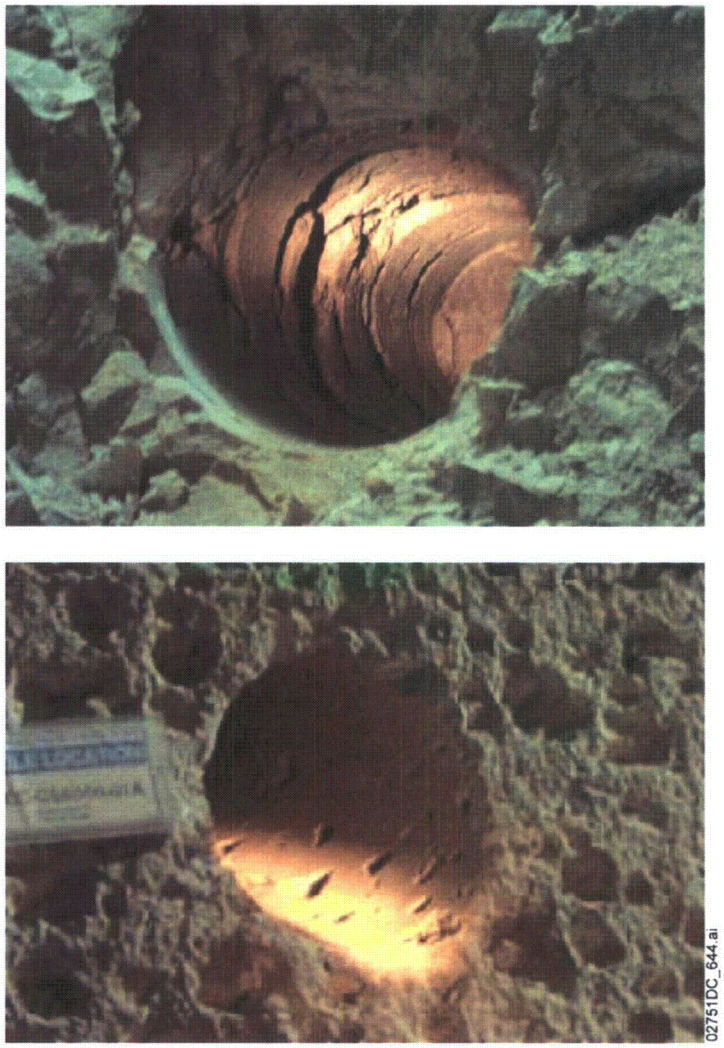

Source: BSC 2004, Figure 7-25.

NOTES: Top photo shows sidewall fracturing/opening of preexisting wall-parallel fractures in a 12-inch-diameter horizontal borehole drilled in the springline of the ESF in low quality Tptpll (approximately Category 1). Overburden depth is approximately 325 m. Depth of fracturing is approximately 1.5 to 2 ft (0.46 to 0.61m).

The bottom photo shows a horizontal, 12-inch-diameter borehole drilled in the springline in good quality Tptpul (approximately Category 5) in the ESF near site of slot test 2 showing no sidewall damage. The depth of overburden is approximately 250 m.

Figure B-11. Observed Rock Mass Conditions at the Tunnel Springline in Lithophysal Rock in the ESF

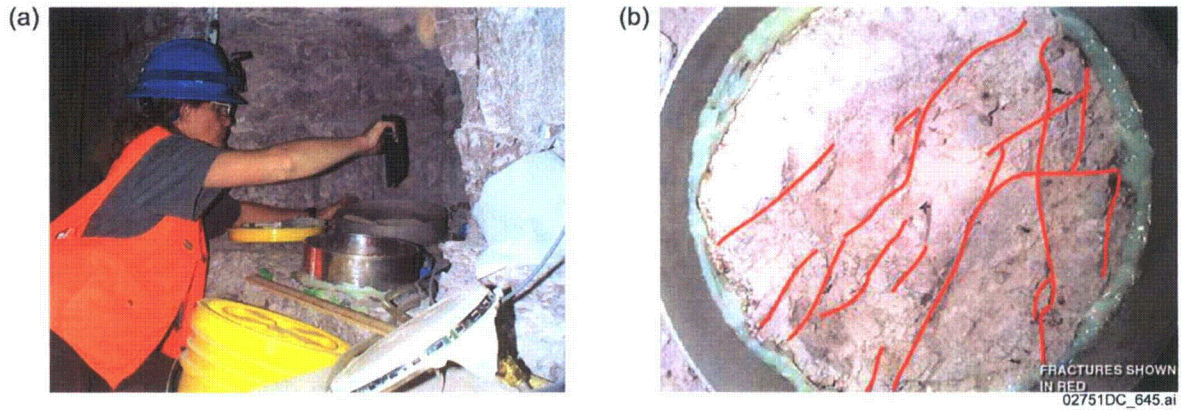

NOTES: Photograph (a) is of the *in situ* unsaturated disk infiltrometer test ECRB Bench 4 in the Tptpll at ECRB Cross Drift station 17+35.

Photograph (b) is of the fractures (red line overlays) mapped in one of the 12-inch-diameter test disks/rings for ECRB Bench 4.

Figure B-12. Infiltration Test ECRB Bench 4 in the Tptpll with Mapped Fractures

B2.6 Sample Management Facility Geologic Logs for the GETC-series Boreholes

In addition to lithostratigraphic and structural descriptions, geologic logs of core from boreholes document the conditions of the core, including the amount of core recovery, piece lengths, and amount of fracturing. Beginning in 1992, the Sample Management Facility (SMF) produced geologic logs for almost all the boreholes in which core was collected, and in addition to lithostratigraphic and structural descriptions, there are two columns that summarize fracture conditions of the core. The column "Piece length" documents the cumulative total intact core pieces that are longer than 0.33 ft (4 inches) in each core run. The column "Frequency" qualitatively documents the fracture frequency (which includes natural and mechanical breaks) by using a six-letter classification code (Table B-5). Classification of "Frequency" is typically for the core run; however, it can be divided into parts of core runs.

Table B-5. Classification Codes for Frequency in SMF Geologic Logs

Code	Title	Description
U	Unfractured	No fractures in core run
V	Very slightly	Most pieces longer than 3 feet
S	Slightly	Core mostly in 1- to 3-foot lengths
M	Moderately	Core mostly in 4-inch to 1-foot lengths
I	Intensely	Pieces average 1 to 4 inches
E	Extremely	Recovery mostly chips and fragments

In 2001 and 2002, a series of boreholes were drilled in the ESF and ECRB Cross Drift for the geotechnical program in support of developing mechanical properties in the repository host horizon lithostratigraphic units (Tptpul, Tptpmn, and Tptpll). These boreholes have identifiers that begin with "ESF-GTEC..." and "ECRB-GTEC...". The GTEC boreholes are 12 inches in diameter and as much as 9 feet deep. The basic fracture information includes both natural and mechanically (drilling) induced fractures; however, one of the significant observations is that there was good core recovery from boreholes in the Tptpul and Tptpmn, but very poor recovery of intact core from boreholes in the Tptpll. Many of the core runs were classified by Frequency as "I" or "E" with a scattered number of "M", and rarely was there a "S". These geologic logs indicate that the Tptpll was readily broken into relatively small blocks during drilling; however: (1) rock itself was drilled very successfully with the tunnel boring machines, (2) the walls of the tunnels throughout most of the Tptpll required very little ground support, and (3) there was very little material that fell from the tunnel walls and crown during the 10 years that tunnels were inspected.

B3 SIGNIFICANT RESULTS FROM FRACTURE DATA

As summarized in this appendix, data on fractures have been collected from numerous studies that document these features in: (1) several locations in the tunnels and surface-based boreholes, (2) different dimensions such as one-dimensional data (length only), two-dimensional data (areas), and locally three-dimensional data (volume), and (3) at a variety of scales from millimeters to hundreds of meters. There are several significant results from these studies:

- Data on fractures from the Tptpll (and other units) are from a variety of locations, including the ESF and ECRB Cross Drift tunnels, surface-based boreholes, and boreholes drilled and slots cut in the walls and invert of the ESF and ECRB Cross Drift; therefore, they represent various spatial and lithostratigraphic conditions of the lithostratigraphic units.

- Fractures occur in many rocks (especially those from the Tptpll) and at many different scales, from tens of meters down to measurements at scales of centimeters and millimeters.

- The most common fracture orientation data in the Tptpll are from DLS and FPGM data, and these fractures have trace lengths greater than 1 m (BSC 2004). Orientation of fractures in the Tptpll from the DLS indicate that most fractures are steeply dipping; however, some are also shallowly dipping (which are referred to as vapor-phase partings), and some are randomly oriented. Orientation of fractures in the Tptpll from the SSF is similar to the total-tunnel DLS data; however, the SSF values are more diverse. At even smaller scales, many fractures in slabs of core and thin sections are steeply dipping; however, fractures of all orientations occur in individual samples.

- The most common fracture trace length data in the Tptpll are from DLS and FPGM data. These fractures typically have trace lengths greater than 1 m (BSC 2004); however, fractures measured at different scales can have a variety of trace lengths. For example, trace lengths of fractures in the SSF data vary from 0.016 to 21.4 m (there was no

minimum trace length) with a mean length of 0.281 m and a median length of 0.140 m. In slabs of core and thin sections, there is an abundance of small trace lengths, many with trace length less than 1 cm.

- The terminations of many fractures can be identified at one or both ends, and although many terminate at (or intersect) other fractures, lithophysae, spots, and even lithic clasts, some fractures terminate in the surrounding rock (or matrix-groundmass). At the scale of the DLS and FPGM data, some fractures transect the entire tunnel, and these would not have identifiable terminations. In the DLS data, about 30% of the fracture terminations are in rock, and in the SSF data, about 36% are in rock. These "termination in rock" relations indicate that about one-third of the fractures are at least partially surrounded by rock bridges. At smaller scales, slabs of core and thin sections indicate two-dimensional fracture networks that are variably developed in specific samples that consist of: (1) fractures connected to other fractures or lithostratigraphic features, and (2) rock bridges between fractures. These data on terminations help identify the overall fabric, including the connectivity of the fracture network and abundance of rock bridges.

- Fractures have identifiable, but typically small, apertures. Aperture values in the DLS and SSF data are typically measured in units of whole millimeters. In the DLS data for the Tptpll in the ECRB Cross Drift, about 44% of the fractures have a maximum aperture of 0 mm and in the SSF about 58% have a maximum aperture of 0 mm. The maximum aperture in the DLS data is 200 mm, and the maximum aperture in the SSF data is 30 mm. At the scale of core and thin sections; apertures are typically measured in parts of millimeters, and in thin section, some apertures are as small as 10 microns. There is no clear relation of aperture to other properties such as trace length, but aperture is helpful to characterize because where it is measureable, there is no strength or cohesion along that segment of the fracture.

- Regardless of two-dimensional configurations of fractures at various scales in the FPGM, DLS, SSF, and even in slabs of core or thin sections, the three-dimensional rock mass of the Tptpll remained intact during the boring of the tunnel, drilling of boreholes, and cutting of core for slabs or thin sections. These conditions support the interpretation that although varying amounts of small-scale features are present and could be activated by mechanical and thermal stresses applied to the rock, the samples are representative of the rock mass.

- Most fractures in the DLS and SSF data from the ECRB Cross Drift, and in the slabs of core and thin sections from surface- and tunnel-based boreholes, are associated with lithostratigraphic features such as vapor-phase minerals, rims, borders, spots, and color of adjacent matrix-groundmass that indicate the fracture and associated features formed during the period of time when the deposit was cooling (BSC 2005). The importance of these observations is that most of the fractures formed during a relatively short period of time after the deposit was formed, and that they are throughout the rock mass.